MedChemComm

RSC Publishing

REVIEW

View Article Online
View Journal | View Issue

Metabolism-guided drug design

Antonia F. Stepan,[a] Vincent Mascitti,[b] Kevin Beaumont[c] and Amit S. Kalgutkar*[c]

Cite this: *Med. Chem. Commun.*, 2013, **4**, 631

Preclinical drug metabolism studies play a key role in the lead identification and optimization process in drug discovery. Characterization of the metabolic pathways of new chemical entities is an integral part of drug discovery not only in optimizing clearance properties but also in eliminating potential safety concerns associated with the formation of protein and/or DNA-reactive metabolites. Metabolism studies in early discovery have been used to identify metabolic soft spots leading to high metabolic instability, and also in the characterization of active metabolites. Availability of such information has aided in the rational design of compounds with increased resistance to metabolism and overall improvements in oral pharmacokinetics and dose size. Mechanistic drug metabolism studies have proven particularly invaluable in mitigating reactive metabolite risks, which can lead to mutagenicity, time-dependent inactivation of cytochrome P450 enzymes and/or idiosyncratic adverse drug reactions. Characterization of stable conjugates derived from bioactivation of small molecule drug candidates provides indirect information on the structure of the reactive metabolite species, thereby providing insight into the bioactivation mechanism and hence a rationale on which to base subsequent chemical intervention strategies. This review will showcase case studies of metabolism-guided drug design using literature and in-house examples.

Received 19th October 2012
Accepted 12th December 2012

DOI: 10.1039/c2md20317k

www.rsc.org/medchemcomm

1 Introduction

The identification of safe and orally efficacious drug candidates amenable to low daily dosing regimens remains a major thrust in most preclinical drug discovery programs across the pharmaceutical industry. Within this arena, drug metabolism research has played an ever increasing role in the identification of drug candidates with the optimal balance of absorption, distribution, metabolism and excretion (ADME) characteristics.[1,2] Arguably, one of the biggest impacts of drug metabolism is in the hit-to-lead stage of drug discovery where many new chemical entities (NCEs) demonstrate metabolic instability in human liver microsomes (HLM), which is principally mediated by the action of cytochrome P450 (CYP) enzymes. The *in vivo* manifestation of high instability is suboptimal pharmacokinetics characterised by plasma clearance (CL_p) values approaching hepatic blood flow, short elimination half-life ($t_{1/2}$) and poor oral bioavailability (F) due to extensive intestinal and first-pass metabolism by CYP enzymes.[3] For human pharmacokinetic predictions (particularly clearance and $t_{1/2}$) in drug discovery, much attention has focused on the role of CYPs, since this particular class of enzymes has been implicated in the metabolism of 60–80% of marketed drugs.[4] For this purpose, most drug discovery programs rely on high throughput screens to monitor the oxidative stability of NCEs in HLM, and to facilitate structure–activity relationship (SAR) studies around oxidative CYP enzymes. The output from such assays allows chemists to design compounds with minimal metabolic turnover in HLM, which scales to low intrinsic clearance (CL_{int}) values for oxidative metabolism in the liver, and ultimately in low predicted human *in vivo* CL_p.[5] The fact that fewer drug candidates attrit in the clinic due to pharmacokinetic related failures is a direct reflection of the positive influence that ADME sciences have had on drug discovery.[3]

While *in vitro* metabolic stability screens provide convenient means for "rank-ordering" large numbers of compounds, information pertaining to the cause of oxidative instability cannot be discerned from such studies and requires customized mechanistic studies including the identification of metabolic "soft spots". As a consequence, detailed metabolite identification studies using state-of-the-art bioanalytical methodology (*e.g.*, liquid chromatography tandem mass spectrometry and NMR) are done more routinely in early discovery, providing invaluable information on how to strategically replace or block metabolically labile sites.[6] Such studies have also proven valuable in the discovery of metabolites with superior pharmacologic potency (relative to the parent compound) and, in some instances, have resulted in the progression of the "active metabolite" as the clinical candidate.

[a]*Neuroscience Medicinal Chemistry, Pfizer Worldwide Research and Development, 700 Main Street, Cambridge, MA 02139, USA*

[b]*Cardiovascular, Metabolic and Endocrine Diseases Medicinal Chemistry, Pfizer Worldwide Research and Development, Eastern Point Road, Groton, CT 06340, USA*

[c]*Pharmacokinetics, Dynamics and Metabolism – New Chemical Entities, Pfizer Worldwide Research and Development, Cambridge, MA 02139, USA. E-mail: amit.kalgutkar@pfizer.com; Tel: +1 617 551 3336*

Although metabolic liability due to CYP enzymes can be prospectively tackled using the above-mentioned strategy, it is possible that NCEs will then be subject to metabolic elimination by non-CYP enzymes that are not represented in liver microsomes. Under such circumstances, when examined *in vivo* in preclinical species, an apparent *in vitro–in vivo* disconnect is revealed (that is, greater *in vivo* CL_p is observed than would be predicted from the *in vitro* metabolic stability studies). The role of non-CYP enzymes in oxidative metabolism has been the subject of several recent reviews.[7–9] Though not an exhaustive list, non-CYP enzymes that consistently reveal themselves as possible contributors to drug metabolism include: (a) monoamine oxidases (MAOs), (b) aldehyde oxidase (AO), (c) uridine glucuronosyl transferases (UGTs) and (d) carboxylesterases. Unfortunately, *in vitro* tools for these enzymes (*e.g.*, liver cytosol, liver S9 and/or hepatocytes) that allow for high throughput screening for non-CYP mediated metabolism and prediction of human pharmacokinetics (specifically CL) are typically not as readily available nor do they possess the fidelity for high confidence prediction of human pharmacokinetics in a similar way that HLM do for CYP enzymes.

In this article, we will highlight examples wherein the results from *in vitro* metabolism studies have been used to guide the design of molecules with increased metabolic stability towards CYP as well as non-CYP enzymes with the goal of modulating CL_p, $t_{1/2}$ and oral *F*. The manuscript will also provide an analysis of rational discovery strategies/approaches towards eliminating metabolism-dependent safety liabilities (*e.g.*, reactive metabolite formation leading to genotoxicity, mechanism-based CYP inactivation and idiosyncratic toxicity) using knowledge gathered from drug metabolism studies. Case studies where biotransformation studies have proven useful in the discovery of active metabolites will also be discussed.

2 Metabolism-guided drug design

General tactics for reducing drug metabolism include, but are not restricted to, reducing lipophilicity, modulating steric and electronic factors, altering stereochemistry and introducing conformational constraints. If a specific site of metabolism is known, then removal of the "soft spot(s)" is usually adopted as a strategy to confer metabolic resistance. Examples of structural modifications to abrogate CYP metabolism are the replacement of a metabolically labile methyl group with the metabolically inert trifluoromethyl substituent, addition of electron-withdrawing fluorine atoms to electron rich phenyl rings to slow the oxidation of the aromatic system or replacement of the metabolically labile group with a bioisostere.[10] In principle, this exercise is not trivial as changes in one parameter can impact other attributes. For instance, attempts to reduce CYP mediated liabilities (*e.g.*, extensive metabolism and/or enzyme inhibition) by decreasing lipophilicity can result in a negative impact on primary pharmacology (*e.g.*, changes in agonist/antagonist behaviour and/or subtype selectivity for target receptor or enzyme) and pharmacokinetics (*e.g.*, poor oral absorption due to increase in polarity). As such, the desired goal in such an exercise is that the SAR for metabolic liability can be optimized in parallel with the SAR required for pharmacological activity and other parameters related to ADME and safety. Of course, it is recognised that changes in one parameter are generally not independent of others, and it is likely that medicinal chemists will ultimately strive to achieve an acceptable balance of properties (for *e.g.*, pharmacokinetics and pharmacodynamics compatible with an acceptable daily dosing regimen and therapeutic margins for safety) rather than optimization of each aspect of the molecule.[11] Drug discovery efforts, which led to the identification of the CCR5 receptor antagonist maraviroc, provide an excellent illustration of these concepts.[12]

2.1 Tactics to modulate metabolism by CYP enzymes

2.1.1 Lowering lipophilicity. In the case of the major constitutively expressed human CYP isoform, *i.e.*, CYP3A4, the predominant interaction with substrates arises from hydrophobic forces as demonstrated from SAR studies and available CYP3A4 crystal structure information.[13–18] The large active site (accessible volume of $\sim$520 $Å^3$) of CYP3A4 is unique among CYP isozymes structurally characterized to date in having seven phenylalanine residues forming a "Phe-cluster", which lie above the heme prosthetic group, with the aromatic side chains stacking against each other to form a hydrophobic core.[13–15] Modulation of physicochemical properties[19–21] such as reduction in molecular weight, lipophilicity (log *P*) or the calculation of the 1-octanol–water partition coefficient (*c*log *P*), the calculated or measured distribution coefficient at pH = 7.4 (*c*log *D* or *E*log *D*) and the reduction in number of hydrogen bond donors and acceptors can therefore confer metabolic resistance into NCEs, independent of the structure and metabolic route. An illustration of such a strategy to attenuate CYP3A4 oxidative instability is evident from SAR studies on a series of *N*-arylsulfonamide-based γ-secretase inhibitors. Lead compound **1** (Fig. 1) suffered from extensive oxidation on the cyclohexyl motif by CYP3A4, which resulted in a short $t_{1/2}$ ($\sim$6 minutes) and a high CL_{int} of 176 mL min^{-1} kg^{-1} in HLM.[22] Reduction in molecular size and introduction of polarity were used as tactics to address the metabolic liability. Indeed, the tetrahydropyran, tetrahydrofuran and oxetane analogs **2**, **3** and **4**, respectively, demonstrated increasing stability ($\uparrow t_{1/2}$ and $\downarrow CL_{int}$) in HLM, which paralleled their intrinsic lipophilicity. Despite the increased stability in HLM, metabolite identification studies revealed that the cycloether ring in compounds **3** and **4** was still prone to oxidative metabolism by CYP3A4 in a similar fashion as the cyclohexyl ring in **1**. On the basis of these observations, it was speculated that the reduction in CL_{int} for the cyclic ethers (especially compounds **3** and **4**) resulted from a diminished affinity for CYP3A4 binding due to a reduction in log *D* and/or unfavourable CYP active site interactions with the ring oxygen, which ultimately translated into a slower rate of metabolism.[22,23]

Another example of modulating oxidative metabolism *via* attenuation of lipophilicity is depicted with a series of aldosterone synthase inhibitors (Fig. 2).[24] Potent enzyme inhibition by the lead compound **5** was offset by a short HLM $t_{1/2}$ due to extensive metabolism on the isobutyl group by CYP enzymes. To

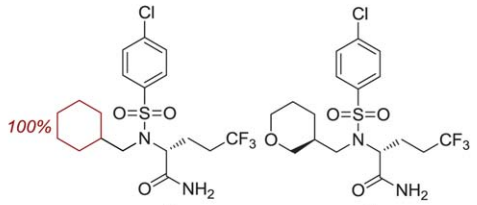

	1	2
ElogD	5.6	3.7
HLM CL_{int} (mL/min/kg)	176	156
IC_{50} ($A\beta_{42}$, nM)	12	45

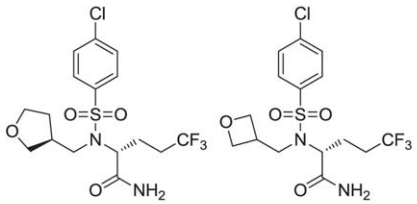

	3	4
ElogD	3.5	2.5
HLM CL_{int} (mL/min/kg)	70	29
IC_{50} ($A\beta_{42}$, nM)	11	16.9

Fig. 1 *In vitro* γ-secretase inhibition and HLM $CL_{int,app}$ data for a representative set of *N*-arylsulfonamides.

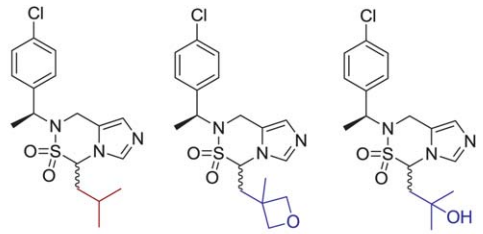

	5	6	7
$clogD_{7.4}$	3.28	2.06	1.69
HLM $t_{1/2}$ (min)	6.0	76	>300
hCYP11B2 IC_{50} (nM)	9.4	7.8	11.4

Fig. 2 *In vitro* potency and HLM stability values of selected aldosterone synthase inhibitors.

mitigate the liability, the isobutyl group in **5** was replaced with an oxetane ring to yield **6**, which demonstrated a greater than 10-fold increase in metabolic stability, while retaining aldosterone synthase inhibitory activity. Additional resistance towards oxidative metabolism was achieved by replacing the oxetane ring with a *tert*-hydroxyl group (compound **7**). The decrease in log *D* coincides with the improvement in metabolic stability of the three analogs.

In a similar fashion, Wan *et al.*[25] reported significant improvements in the mouse liver metabolic stability with some 11β-hydroxysteroid dehydrogenase type 1 (11β-HSD1) inhibitors (exemplified by piperidine and morpholine derivatives **8** and **9**,

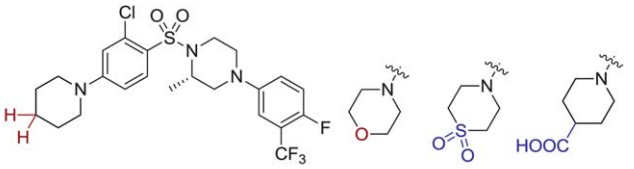

	8	9	10	11
$logD_{7.4}$	5.90	4.28	3.08	1.97
MLM $t_{1/2}$ (min)	6.0	14	>30	>30
HLM $t_{1/2}$ (min)	21	>30	>30	>30
11β-HSD1 IC_{50} (nM)	97	10	10	10

Fig. 3 *In vitro* 11β-HSD1 activity, MLM and HLM stability of selected compounds.

respectively) *via* inclusion of polar functionalities into the ring systems (Fig. 3). Both the thiomorpholine 1,1-dioxide (**10**) and the isonipecotic acid (**11**) derivatives possess lower log *D* values, which may explain the increase in oxidative stability in HLM as well as mouse liver microsomes (MLM). As such, compound **11** also retained the 11β-HSD1 potency discerned with the lead compound **9**, while demonstrating excellent oral pharmacokinetics ($CL_p = 9$ mL min^{-1} kg^{-1}, oral $F = 100\%$) in the mouse.

2.1.2 Modifying the site of metabolism. An example of metabolic blocking strategy to minimize oxidative metabolism is evident in SAR work on human immunodeficiency virus (HIV) protease inhibitors for the treatment of HIV-1 infections. As a structural class, protease inhibitors, exemplified by indinavir, generally suffer from extensive first-pass CYP3A-mediated metabolism in the small intestine and liver. Attempts to develop agents with improved pharmacokinetics focused on blocking the sites of CYP3A4-mediated metabolism. For instance, indinavir undergoes metabolism in two regions of the molecule designated as P_2' and P_3 (Fig. 4). Specifically, oxidation takes

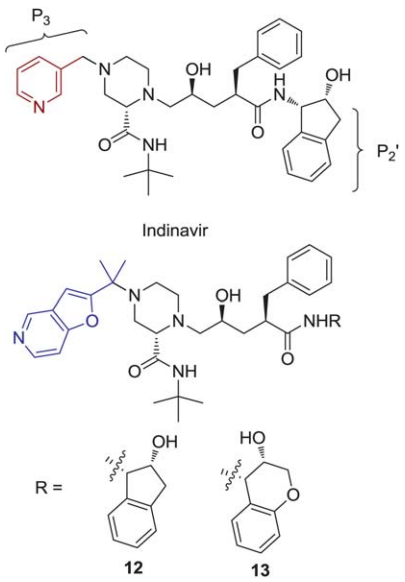

Fig. 4 Improving oxidative metabolic stability in the HIV-1 protease inhibitor indinavir *via* structural modifications of metabolic "soft spots".

place at the benzylic position of the aminoindanol moiety (P_2'), in addition to the methylene linker (P_3). In an attempt to improve CL, Cheng *et al.*[26] incorporated a *gem*-dimethyl and pyridylfuran functionalities in P_3 (compound **12**), along with replacement of the aminoindanol with an aminochromanol moiety (compound **13**). This led to analogues that displayed enhanced activity (relative to indinavir) in primary *in vitro* pharmacology assays. Compound **12** also demonstrated a two-fold increase in terminal $t_{1/2}$ (relative to indinavir) in rats and dogs.

The calcium channel blocker diltiazem (**14**, Fig. 5) is extensively metabolized *via* distinct pathways that include *N*-demethylation, ester hydrolysis and *O*-demethylation. The enzyme responsible for the major route (*N*-demethylation) of clearance has been shown to be CYP3A4. Although widely used in therapy, diltiazem has a relatively short duration of action. In the search for metabolically resistant analogues, Floyd *et al.*[27] substituted the benzothiazepinone motif in **14** with the trifluoromethyl benzazepinone ring structure to give lead analog **15**. Metabolite identification studies in rat liver microsomes (RLM) indicated that the principal elimination pathways of **15** were similar to that of **14** with deamination, *N*-demethylation, acetate hydrolysis and *O*-demethylation all occurring. Interestingly, the *N*-desmethyl metabolite **16** was pharmacologically equipotent to the parent molecule **15**, and was itself stable to oxidative deamination. This prompted the design of the *N*-1-pyrrolidinyl derivative **17**, which maintained the *in vitro* potency, and metabolic stability of **16**. Because the rate-limiting step in the CYP-mediated oxidative deamination involves the abstraction of an electron from the nitrogen lone pair,[28] a potential explanation for the increased metabolic stability of **16** and **17** (relative to **15**) is that radical formation from secondary amines is a less favoured process compared to tertiary amines due to the increase in secondary amine basicity. As indicated by the calculated values of log $D_{7.4}$, the decrease in overall lipophilicity may have also contributed to the improved metabolic profiles of **16** and **17**, respectively.

In the course of lead optimization of a second generation of imidazolopiperazine-based antimalarial agents, lead compound **18** (Fig. 6) demonstrated inferior *in vivo* efficacy when administered orally to mice.[29] Metabolite identification studies in MLM and HLM revealed the formation of two cyclised metabolites **20** and **21**, arising from the oxidation of the piperazine ring to an intermediate carbinol amide species **19** (Fig. 6). Incorporation of 8,8-*gem*-dimethyl group on the piperazine ring led to derivatives (*e.g.*, compound **22**) with significant improvements in potency, *in vitro* metabolic stability profile and, as a result, enhanced oral exposure in mice, which is reflected in the reduced ED_{99} values for **22**.

2.1.3 Incorporation of fluorine. The effect of fluorine on the ADME profile of compounds has been known and exploited by medicinal chemists for some time,[30] substituting hydrogen with fluorine at metabolically labile positions is a common approach to attenuate metabolism. The tactic relies on the powerful electron withdrawing effects of fluorine and the strength of the C–F bond which, at approximately 108 kcal mol^{-1}, is the strongest bond known between carbon and any other atom.[10,31,32] This phenomenon renders the C–F bond chemically inert under most biological conditions. Moorjani *et al.*[33] reported on the use of fluorine substitution to enhance metabolic stability in a series of non-xanthine selective A_{2A} antagonists for the potential treatment of Parkinson's disease. Lead compound **23** (Fig. 7) demonstrated good antagonist activity but was unstable in HLM (compound **23:** $CL_{int} = 54$ mL min^{-1} kg^{-1}). Introduction of a fluorine atom in the aromatic ring of **23** gave analog **24**, which showed significant improvements in metabolic stability (compound **24:** $CL_{int} = 3$ mL min^{-1} kg^{-1}) while exhibiting single digit nanomolar potency for the A_{2A} receptor. In this scenario, the electron withdrawing effects

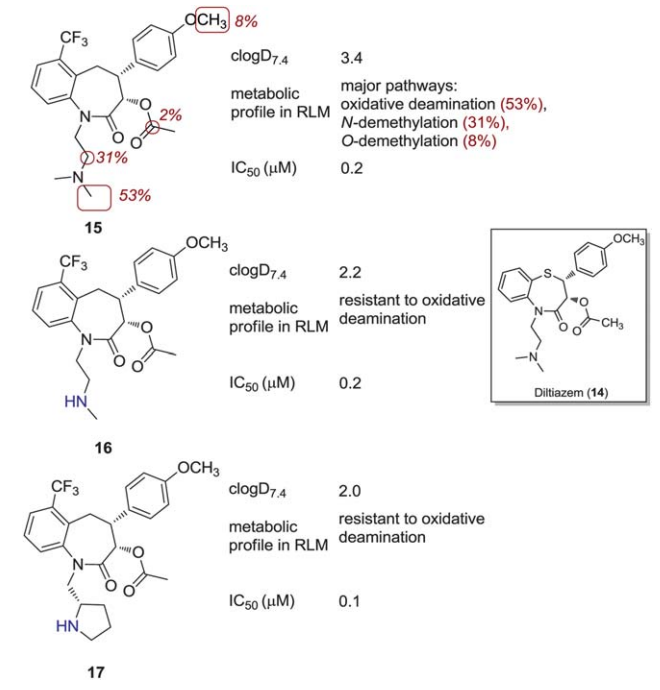

Fig. 5 Increasing resistance towards oxidative deamination in the diltiazem analog **15** by increasing the basicity of the metabolic soft spot.

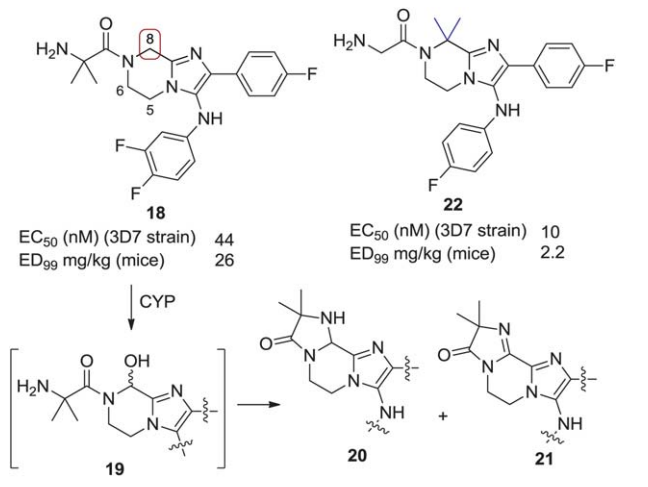

Fig. 6 Circumventing metabolic instability on a piperazine ring as illustrated with imidazolopiperazine-based antimalarial agents.

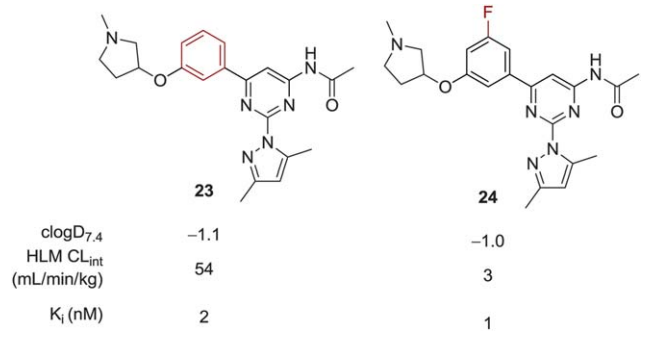

Fig. 7 Increasing metabolic stability through the use of the fluorine atom as illustrated with the A_{2A} antagonist **24** for the potential treatment of Parkinson's disease.

of the fluorine atom rendered the phenyl group more resistant to CYP oxidation without significantly reducing the overall polarity of the molecule (compound **24:** *c*log $D_{7.4} = -1.0$; compound **23:** *c*log $D_{7.4} = -1.1$).

Pfizer medicinal chemists in the context of their GPR119 program[34] also reported an additional example of CL reduction mediated by the introduction of a fluorine-containing stereocenter. The design capitalized on the conformational restriction found in *N*-β-fluoroethylamide derivatives to help maintain good levels of potency while driving down both lipophilicity and CL_{int} due to oxidative metabolism in HLM (compounds **25** and **26**, Fig. 8).

Another example relates to the metabolism-directed lead optimization of *N*-(3,3-diphenyl-propyl)nicotinamide (**27**) (Fig. 9), a potent inhibitor of soluble epoxide hydrolase (sEH).[35] Metabolic stability examination of **27** revealed a short metabolic $t_{1/2}$ in HLM and RLM due to its high lipophilicity. Metabolite identification studies indicated extensive hydroxylation on the pendant phenyl groups of the benzhydryl motif, which prompted the design of the corresponding bis-(4-fluorophenyl) analog **28** in order to block the metabolically vulnerable sites with fluorine atoms. Examination of the *in vitro* metabolic profile of **28**, however, revealed an apparent metabolic switch in the major route of metabolism to pyridine ring hydroxylation, a feature that was consistent with a lack of change in microsomal half-lives. Hypothesizing that substituents on the pyridine ring could slow metabolism, analogues such as **29** were synthesized. Compound **29** retained the sEH inhibitory potency of **28**, and was practically inert to oxidative metabolism in both human and rat liver microsomes. However, **29** revealed poor *in vivo* oral absorption in rats due to its poor aqueous solubility driven by

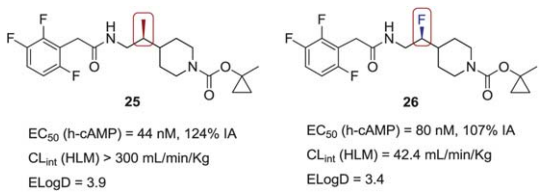

Fig. 8 Reduction in CL_{int} through the use of fluorine in a series of *N*-β-fluoroethylamide GPR119 receptor agonists.

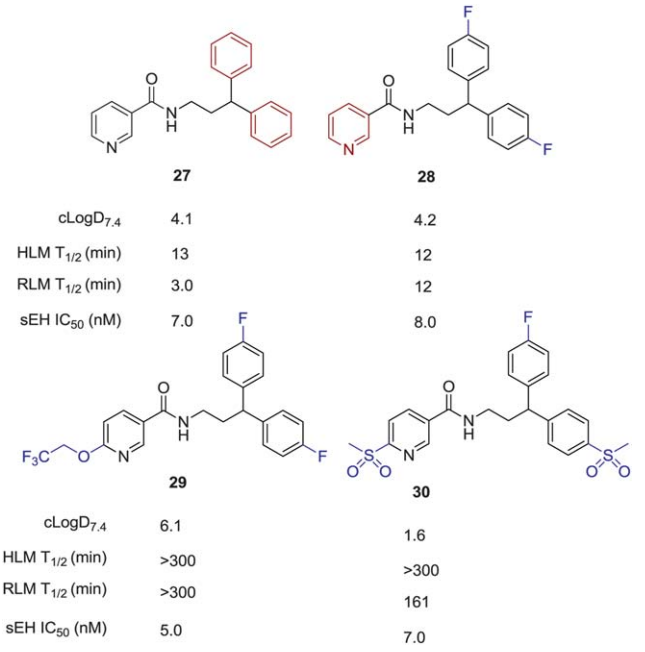

Fig. 9 Optimization of arylamides as inhibitors of sEH.

its very high lipophilic nature. Guided by the analysis of the co-structure of **27** with sEH, one fluorine atom in **29** was substituted for an additional polar substituent on the right-hand side benzhydryl motif with simultaneous modifications on the pyridine ring to balance physicochemical properties in order to increase oral absorption. Overall, this example illustrates how the combination of both tactics, namely reduction of lipophilicity and blockade of metabolic soft spot(s) through the use of fluorine, was used in concert to identify potent and *in vitro* metabolically stable epoxide hydrolase inhibitors with excellent oral absorption as highlighted with compound **30**.

Burgey *et al.*[36] also reported on the metabolism-directed optimization of a series of 3-(2-phenethylamino)-6-methylpyrazinone acetamide thrombin inhibitors (exemplified by compound **31**, Fig. 10), which involved the use of fluorine atoms to stabilize oxidative metabolism. Metabolic profiling of **31** revealed three principal sites of metabolism involving oxidation

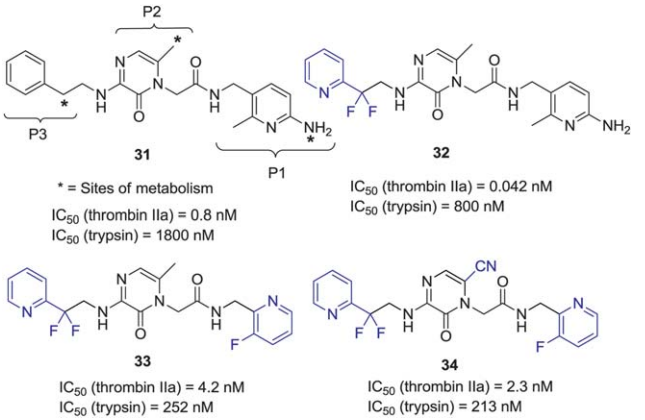

Fig. 10 Modulation of oxidative metabolism in thrombin inhibitors.

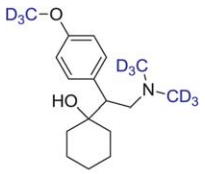

SD-254 (**35**)

Fig. 11 Deuteration of venlafaxine as a strategy to reduce interindividual variability in pharmacokinetics.

of the P3 and P2 regions and phase II conjugation of the P1 basic amino group. A study to examine the effect of P3 benzylic substitution on thrombin inhibitory potency was initiated with the goal of sterically blocking oxidative metabolism. Incorporation of a 2-pyridyl and *gem*-difluoro modifications afforded **32** with improved thrombin inhibitory potency and lack of metabolic soft spots at the P3 region. Attempts to address phase II metabolism in **31** *via* removal of the amino group (susceptible to glucuronidation), however, led to a dramatic loss of thrombin inhibitory potency. Additional SAR studies on suitable 2-aminopyridine replacements in the P1 region led to the identification of the *meta*-fluoropyridyl substituent that abrogated the glucuronidation liability while maintaining inhibitory potency in the targeted range for efficacy (compound **33**). Metabolism of the P2 benzylic group was finally addressed *via* replacement of the problematic methyl group with a cyano functionality leading to compound **34** with excellent pharmacology and animal pharmacokinetics.

2.1.4 Incorporation of deuterium. An appreciation of kinetic deuterium isotope effects has led to an increased awareness that deuteration can be a useful approach to improve the pharmacokinetic properties of drug candidates. The strategic incorporation of deuterium at sites of metabolism where hydrogen atom abstraction is the rate-determining step can potentially impede metabolism and redirect metabolic pathways. In some cases, the rate of metabolism *via* a specific pathway may be attenuated, but the rate of overall substrate consumption or overall clearance is not significantly altered, due to a compensatory increase in the rate of formation of an alternate metabolite.[37] However, as will be discussed later, a more appropriate application of the deuteration strategy is in mitigating CYP inhibition risks. An example where deuteration can attenuate metabolism is evident with SD-254 (**35**), the deuterated form of the anti-depressant venlafaxine (Fig. 11).[38] Venlafaxine is prone to *O*-demethylation as the major metabolic pathway in humans, with *N*-demethylation playing a minor role. The metabolism of venlafaxine is mediated by polymorphic CYP2D6 and CYP2C19, which leads to significant interindividual variability in human pharmacokinetics. Deuteration reduces the rate of metabolism of **35** by ~50%, which leads to increased exposure of the parent drug in humans, and less variability in pharmacokinetics.

2.2 Tactics to modulate metabolism by non-CYP enzymes

2.2.1 Aldehyde oxidase. Aldehyde oxidase (AO) contains a molybdenum pyranopterin cofactor (MoCo) (Fig. 12) that

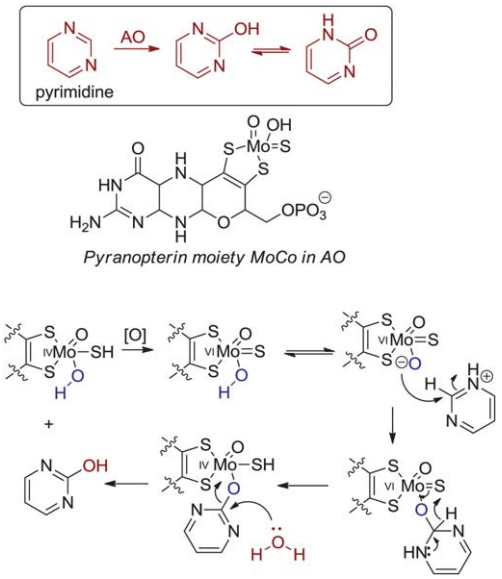

Fig. 12 Mechanism of AO mediated oxidation of heterocyclic rings.

catalyzes the α- or γ-carbon oxidation of imines ($R_1R_2C{=}NR_3$) in nitrogen-containing heterocycles (*e.g.*, pyridine, pyrimidine, quinoline, quinoxaline, *etc.*), resulting in the formation of the corresponding lactam (α-carbon oxidation) or aminoenone (γ-carbon oxidation) metabolites, respectively, as illustrated with the simple heterocycle pyrimidine (Fig. 12).[8] AO is located in the cytosol of cells and incorporates the oxygen into the product *via* a nucleophilic addition-like mechanism (Fig. 12). In a typical catalytic cycle, the heterocyclic substrate is oxidized at the Mo center. The reducing equivalents are passed to flavin adenine dinucleotide, which is then reoxidized by molecular oxygen. Both CYP and AO enzymes utilize molecular oxygen as the ultimate electron acceptor. However, the oxygen atom that is incorporated into the product during AO-mediated oxidative hydroxylation is derived from water and not oxygen. As such, the oxidative hydroxylation of substrates by AO is complementary to that mediated by CYP enzymes. Thus, design approaches to confer CYP resistance into aromatic rings by introducing polar heteroatoms can potentially introduce oxidative liability by AO. Successful strategies to eliminate or reduce AO metabolism include removal of the electron deficient imine, changing the positions of the heteroatoms in the ring, increasing electron density or sterics around the vulnerable site or altering the molecules at remote locations to reduce binding affinities to AO.

The disclosure of novel azetidinyl ketolides for the treatment for multidrug resistant respiratory tract infections by Magee *et al.* highlights some of these tactics to circumvent AO metabolism.[39] A series of heterocycle-substituted azetidinyl ketolide derivatives were identified as potent antibacterial agents with minimal oxidative turnover in HLM. Compound **36** (Fig. 13) was predicted to have low human CL_p by scaling of HLM CL_{int}, which combined with its attractive pharmacologic profile led to its advancement into first-in-human trials. However, upon oral dosing in the predicted efficacious dose range of 300–1000 mg, the measured plasma exposures were

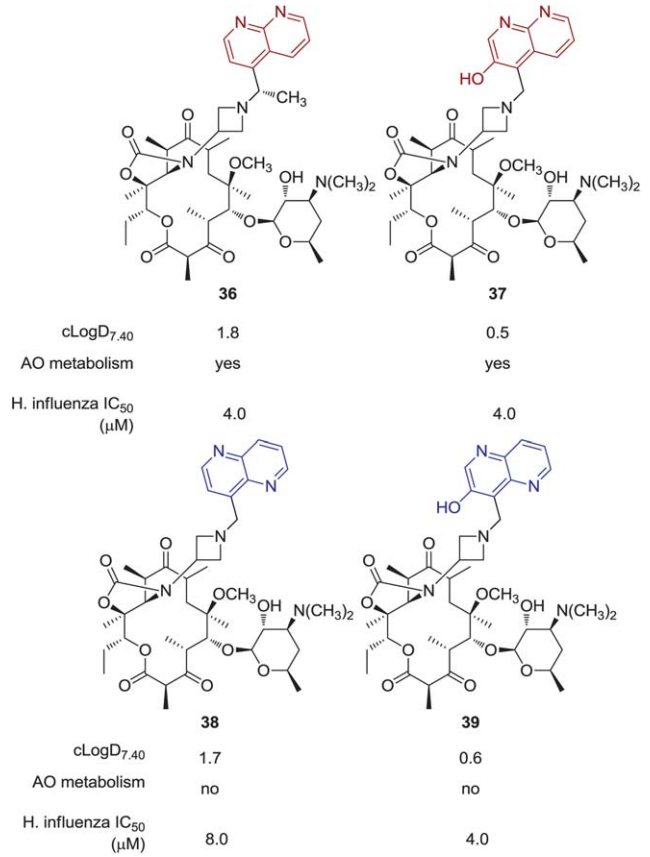

Fig. 13 SAR for AO mediated oxidation of azetidinyl ketolide derivatives.

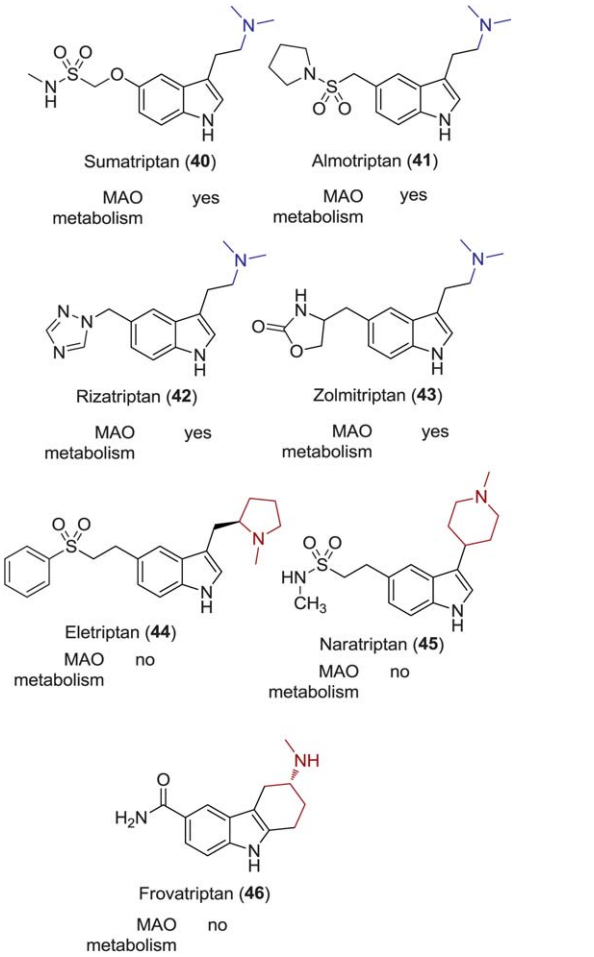

Fig. 14 SAR for oxidative deamination of the triptan class of anti-migraine drugs by MAO-A.

~20% of the predicted area under the plasma concentration time curve values, leading to the termination of further clinical investigation with the agent. Incubation of **36** in human liver cytosol in the presence or absence of raloxifene (a selective inhibitor of AO) revealed that the 1,8-naphthyridine ring system was hydroxylated by AO (the regiochemistry of hydroxylation was not established). As highlighted with **37** (metabolized by AO) and **38** (not metabolized by AO), the AO liability was not circumvented by incorporation of polar functionalities such as the hydroxyl group despite a reduction in lipophilicity. However, modification of the heteroatom arrangement deferred oxidation by AO (compounds **38** and **39**). Compound **38** had the best overall profile, and was advanced into phase I clinical trials. Additional examples of drug design strategies to rectify AO liabilities are presented in the review article by Pryde *et al.*[8]

2.2.2 Monoamine oxidases. Monoamine oxidase (MAO) isoforms A and B are found in the outer membrane of mitochondria in most cell types in the body and catalyze the oxidative deamination of structurally diverse alkyl- and arylalkyl amines.[7,9] Elaborate SAR studies suggest that MAO-A and -B are efficient catalysts especially for amines that are 1–3 carbons away from an aryl group. Although primary and secondary amines are deaminated indiscriminately by both isozymes, tertiary amines generally display selectivity toward one form of the enzyme. MAO-A is the principal enzyme responsible for the clearance of acyclic tertiary amines sumatriptan (**40**), almotriptan (**41**) and rizatriptan (**42**) (Fig. 14) leading to the formation of the corresponding indoleacetic acid metabolites.[40–42] The structurally related zolmitriptan (**43**) is cleared in humans primarily *via* *N*-demethylation and *N*-oxidation that is mediated by CYP1A2. The *N*-demethylated metabolite undergoes selective MAO-A-catalyzed oxidation to yield the analogous indole acetic acid derivative.[43]

Despite structural similarity, the cyclic tertiary amines eletriptan (**44**) and naratriptan (**45**) and the secondary amine frovatriptan (**46**) are not substrates of MAO-A and/or MAO-B. Compounds **44** and **46** are metabolized by CYP enzymes,[44,45] whereas **45** is predominantly eliminated in the urine in unchanged form (naratriptan product information). The $t_{1/2}$ of compounds **44–46** is from 26–30 hours, and is longer than that of sumatriptan (~2 hours).[46] Whether the medicinal chemistry tactics (conversion of an acyclic tertiary amine motif to a cyclic tertiary amine motif) adopted to eliminate the MAO metabolism component in sumatriptan and almotriptan to yield non-MAO substrates like eletriptan and naratriptan can be applied universally remains to be studied with additional examples. Also, it is important to note that most basic amine drugs do not have MAO-catalyzed metabolism as a primary clearance pathway with the exception of the triptans. The findings are probably a reflection of their relatively low lipophilicity (*e.g.*, the

log $D_{7.4}$ value of sumatriptan is −1.7) and stability towards CYP enzymes. Consequently, given their structural similarity with the endogenous neurotransmitter serotonin, which is a preferred MAO-A substrate, it is not altogether surprising that several of the triptans ultimately succumb to metabolism by MAO-A.[9]

2.2.3 Phase II conjugating enzymes. Conjugation with glucuronic acid or sulfate requires a nucleophilic site in the molecule. Substrates for uridine 5′-diphospho-glucuronosyltransferase (UGT) include phenols, primary, secondary or even tertiary alcohols and amines, carboxylic acids and heterocycles such as pyrazoles, whereas substrates for sulfation catalyzed by sulfotransferases (SULTs) usually contain a phenolic functionality.[47] In some cases primary alcohols can also form sulfate conjugates. For instance, the peroxisome proliferator-activated receptor γ (PPAR-γ) agonist troglitazone (Fig. 15) is principally metabolised in man *via* sulphation of its phenol group.[48] It is interesting to note that both troglitazone and its sulphate metabolite are potent inhibitors of bile salt export pump, which may account for the cholestatic mechanism associated with troglitazone liver injury.[49] Related PPAR-γ agonists pioglitazone and rosiglitazone (see Fig. 15) do not contain the phenol and are not subject to sulphation. Interestingly, both compounds are also devoid of cholestasis observed with troglitazone. It is also noteworthy to point out that pioglitazone and rosiglitazone are significantly more potent as PPAR-γ agonists (relative to troglitazone) indicating that the phenol motif is not essential for primary pharmacology. The take home message based on the PPAR tale is to eliminate unnecessary phase II metabolic soft spots on lead chemical matter unless absolutely needed for primary pharmacology.

Tactics to attenuate glucuronidation are evident in SAR studies on a second generation of *N*-hydroxyurea-based 5-lipoxygenase (5-LO) inhibitors, wherein the duration of 5-LO inhibition after oral administration in animals was optimized by reducing glucuronidation of the *N*-hydroxyurea motif.[50,51] The primary route of metabolism of zileuton (Fig. 16), the first *N*-hydroxyurea-based 5-LO inhibitor, involves *O*-glucuronidation of the *N*-hydroxyurea group, resulting in a relatively short plasma $t_{1/2}$ of ~3 hours after oral dosing in humans.[52] Clinical trials with zileuton in asthmatics demonstrated efficacy with oral administration of 600 mg four times daily. Validation of the therapeutic application of 5-LO inhibitors in asthma patients has provided an impetus to identify an optimized compound with greater potency and longer duration of action that would in turn provide a lower and less frequent daily dose. The duration of 5-LO inhibition after oral administration in monkeys (as a model for human pharmacokinetics) was optimized by identification of structural features in the proximity of the *N*-hydroxyurea (*e.g.*, compounds **47** and **48**), which correlated with low *in vitro* glucuronidation rates.[51] For instance, compound **48** (phenoxyheterocyclic-substituted template in combination with the butynyl link) proved to be a compatible match that enhanced inhibitory potency and provided resistance to glucuronidation, resulting in a long $t_{1/2}$ in monkeys.

An additional example of structural modifications aimed at reduction of phase II glucuronidation has also been reported by Mascitti *et al.* during their evaluation of a series of C-5 spirocyclic *C*-glucoside SGLT2 inhibitors, such as compound **49** (Fig. 17).[53] Interestingly, replacement of the oxetane ring in **49** by an azetidine, as in **50**, produced a compound of similar lipophilicity but with markedly reduced CL_{int} in human hepatocytes (HHEP) compared to **49**. Mindful of this observation, it was proposed that the increased glucuronidation in **49** was due to a lack of an H-bond donor or polar group at the C-5 position. This hypothesis appeared to be corroborated by the fact that

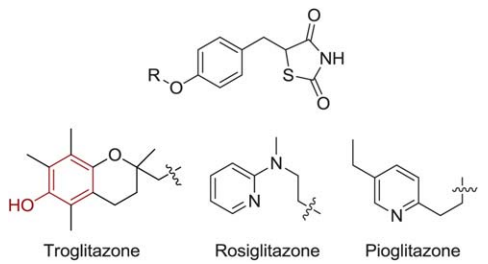

Fig. 15 Structures of the PPAR-γ agonists.

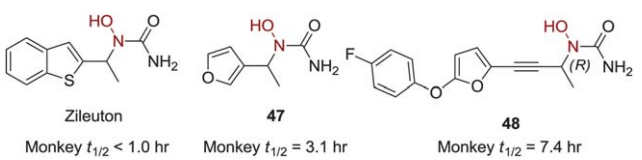

Fig. 16 Strategies to reduce glucuronidation rates in a series of 5-LO inhibitors.

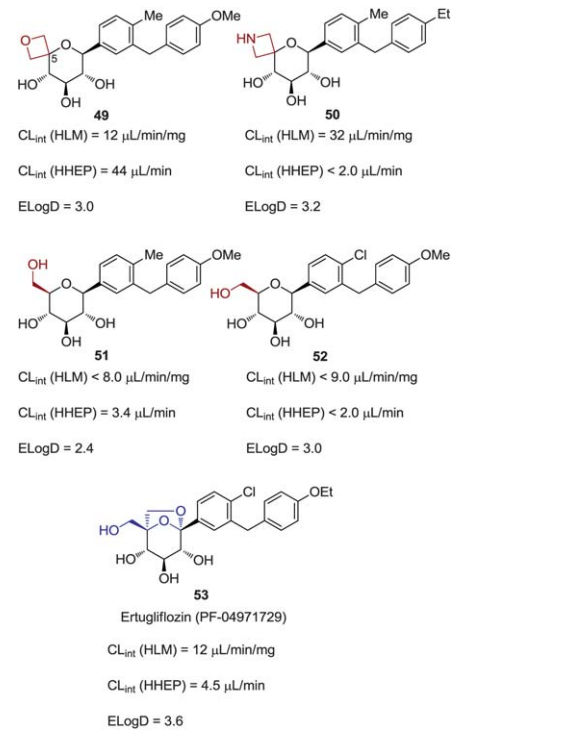

Fig. 17 Attenuating glucuronidation in a series of SGLT2 inhibitors. HHEP CL_{int} values are expressed per million cells.

C-aryl glucosides of similar lipophilicities, such as **51** and **52**, have a reduced CL_{int} (~2.0 to 4.0 μL min^{-1} per million cells) in HHEP. These efforts ultimately led to the identification of the antidiabetic agent ertugliflozin (PF-04971729; **53**), which demonstrated very low turnover *in vitro* in HLM and HHEP; these findings were corroborated during first-in-human trials, where **53** demonstrated low CL_p in humans upon oral dosing.[54]

2.2.4 Amidases/esterases. Non-specific esterases are distributed widely throughout the body. The activity of these enzymes varies markedly with different tissues. In mammals the highest levels are found in the liver and the kidney. Rodent blood (and plasma) has a very high esterase content (relative to dog and human), and may give a misleading view of stability if this species is used in isolation.[55] While esterases have proven useful in prodrug design,[56] there are scenarios wherein unwarranted cleavage of amide (or ester) bonds in lead chemical matter could occur in preclinical species and/or humans, leading to higher than anticipated plasma CL.[57]

An interesting case study highlighting a strategy to mitigate hydrolytic instability was recently disclosed in a discovery program attempting to identify orally active factor Xa inhibitors as potential anticoagulant agents.[58] Lead compound **54** (Fig. 18) underwent a facile hydrolysis in HLM (in the absence of CYP cofactor NADPH) to yield carboxylic acid **55** (~23%) as an inactive metabolite. In contrast, **54** displayed complete resistance towards hydrolytic cleavage in monkeys. The observation that hydrolytic instability was species dependent meant that human pharmacokinetics would be difficult to predict. In addition, these observations raised potential concerns regarding the formation of human specific metabolites, on the basis of which Fujimoto *et al.* focused on identifying factor Xa inhibitors with improved stability towards hydrolysis in human hepatic tissue. The efforts were largely facilitated by metabolite identification studies on **54**, which revealed the formation of active metabolites, namely the α-hydroxy (**56a**/**56b**) and hydroxymethyl derivative **57** (Fig. 18), upon oral administration to monkeys and in human hepatic tissue. Incidentally, compounds **56a**/**56b** were significantly more resistant to hydrolysis in HLM, suggesting that the introduction of the hydroxyl group at the α-position disfavoured the cleavage of the amide bond. In addition, molecular docking studies utilizing the crystal structure of factor Xa revealed that the imidazoimidazolone ring in **56a** was only involved in hydrophobic interactions in the protein, and could be replaced with other smaller bicyclic and monocyclic rings.[59] Consequently, further SAR studies aimed at small ring replacements in **56a** resulted in the identification of the tetrahydropyrimidin-2(1*H*)-one derivative TAK-442 (compound **58**) as a potent and selective factor Xa inhibitor, currently in clinical trials. Compound **58** showed no amide bond hydrolysis in HLM and exhibited a favourable pharmacokinetic/pharmacodynamic profile in preclinical species.

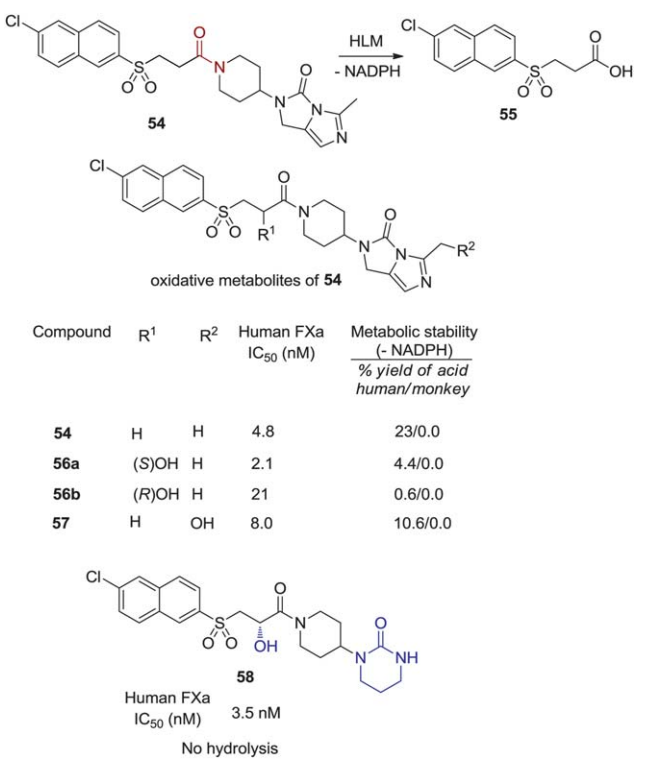

Compound	R^1	R^2	Human FXa IC_{50} (nM)	Metabolic stability (- NADPH) % yield of acid human/monkey
54	H	H	4.8	23/0.0
56a	(*S*)OH	H	2.1	4.4/0.0
56b	(*R*)OH	H	21	0.6/0.0
57	H	OH	8.0	10.6/0.0

Fig. 18 A metabolism-guided strategy to eliminate hydrolytic instability in a series of factor Xa inhibitors.

3 Metabolism-guided design of short-acting drugs

While optimization of ADME attributes usually focuses on reducing CL and increasing half-lives, in some scenarios (*e.g.*, mechanism-based safety concerns), engagement of the pharmacologic target requires short-acting agents and/or molecules with specific CL and $t_{1/2}$ values. Metabolism-guided drug design has also proven very valuable in such efforts. For instance, the known lability of benzylic positions on electron rich heteroatoms towards CYP metabolism has been exploited to decrease the unacceptably low clearance and resultant long half-life of some selective cyclooxygenase-2 inhibitor lead compounds. Specifically, the anti-inflammatory agent celecoxib (Fig. 19) exhibits a $t_{1/2}$ of 3.5 hours in rats, whereas early structural leads, represented by compounds in which celecoxib's benzylic methyl were replaced with a halogen substituent (*e.g.*, compound **59**, Fig. 19), possessed $t_{1/2}$ values >220 hours in rats.[60]

In another illustration, short-acting calcium-sensing receptor antagonists were designed by incorporating the metabolically labile thiomethyl functionality into the metabolically stable, zwitterionic amino alcohol leads (*e.g.*, compound **60**, Fig. 19) to increase oxidative clearance by CYP3A4, while delivering a pharmacologically inactive sulfoxide metabolite. The efforts led to the discovery of clinical candidates **61** and **62** for the potential treatment of osteoporosis.[61]

In a slightly different approach, while working on a series of serotonin re-uptake inhibitors, Middleton *et al.*[62] reported a strategy aimed at purposely redirecting metabolism away from a specific site. Lead compound **63** (Fig. 19), although a promising lead, was found to undergo CYP2D6-mediated *N*-demethylation to the secondary amine metabolite, which was both pharmacologically active and possessed a relatively long $t_{1/2}$, a phenomenon that was inconsistent with the objectives of this

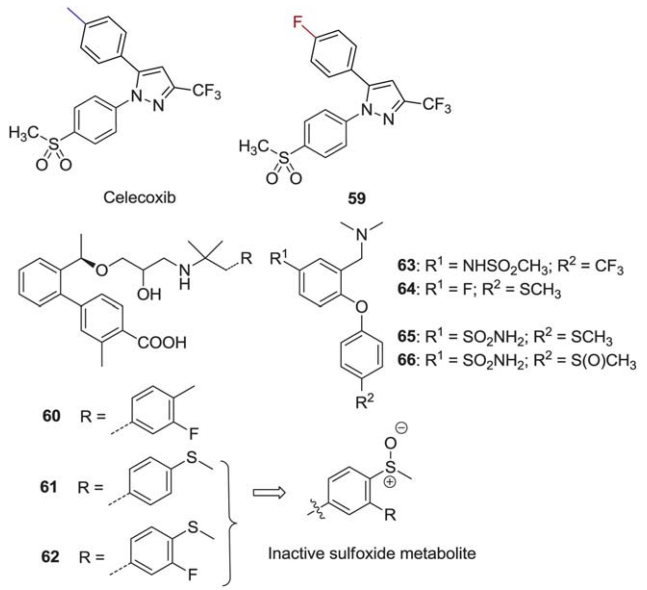

Fig. 19 Metabolism-guided strategies to enable the design of short-acting clinical agents.

program. A simple thiomethyl analog **64** was designed to explore if CYP-mediated thio alkyl *S*-oxidation could be a rapid metabolic process that could compete with *N*-demethylation. Further expansion of the SAR led to the sulfonamide **65**, which was potent and selective for serotonin over dopamine and noradrenaline re-uptake inhibition. *In vitro*, the sulfoxide **66** was the predominant metabolite (>90%) and showed only weak pharmacological activity (IC_{50} > 1 μM). *In vivo*, in both rat and dog pharmacokinetic studies, the parent compound **65** retained the desired ADME properties of **63** and as predicted by the *in vitro* studies, the sulfoxide **66** was the predominant metabolite. Compound **65** possessed the desired short $t_{1/2}$ and was shown to be inactive against a broad panel of other receptors, enzymes and ion channels. Based on its profile, sulfonamide **65** was progressed into clinical development.

4 Eliminating reactive metabolite liabilities in drug design

Metabolic activation (also referred to as bioactivation) of innate functional groups into electrophilic reactive metabolites is considered to be an undesirable trait of drug candidates on the grounds of evidence linking this liability with genotoxicity,[63] drug–drug interactions (DDI),[64] end-organ toxicity and immune-mediated idiosyncratic adverse drug reactions (IADRs).[65–67] Most pharmaceutical companies have implemented guidelines/procedures to evaluate the potential of a drug candidate to form reactive metabolites with the goal of eliminating or minimizing this liability by rational structural modifications. General avoidance of functional groups that have been associated with reactive metabolite formation (referred to as "structural alerts")[65] is almost a norm in drug design, particularly at the lead optimization/candidate selection stage. As such, qualitative assessment of CYP-mediated reactive metabolite formation *in vitro* usually involves "trapping" studies conducted with NADPH-supplemented HLM in the presence of reduced glutathione (GSH), amines (*e.g.*, semicarbazide and methoxylamine) and/or cyanide ion. Microsomes can be replaced by alternate metabolism systems (*e.g.*, liver cytosol, liver S-9 fractions, hepatocytes, *etc.*) to evaluate the participation of non-CYP enzymes in reactive metabolite formation. In the case of reactive metabolite positives, characterization of the nucleophile-reactive metabolite structure provides insight into the structure of the reactive intermediate and the mechanism leading to its formation. The information is then used, as appropriate, to modify the structure of the reactive metabolite positives in order to eliminate the liability.

4.1 Eliminating metabolism-dependent mutagenicity

The role of metabolism in generating reactive metabolites capable of covalently adducting with nucleic acids and leading to mutagenic lesions is well established for many endogenous and exogenous xenobiotics (including drugs). Virtually any molecule that forms reactive species possesses the propensity to modify DNA and elicit a genotoxic/carcinogenic response. Genetic toxicology testing is usually conducted in the early stages of drug development with the intent of identifying hazards associated with both the parent molecule and its metabolites. Identification of genotoxic metabolites in *in vitro* test systems is accomplished by employing metabolic activation systems (*e.g.*, Aroclor 1254-induced rat liver S9). The *Salmonella* reverse mutation assay has become an integral part of the safety evaluation of drug candidates and is required by regulatory agencies for drug approvals worldwide. The mutagenic potential of small molecule drug candidates is generally evaluated in genetically different strains of the *Salmonella typhimurium*, such as TA98, TA100, TA1535, and TA1537. These test strains all carry some type of defective (mutant) gene that prevents them from synthesizing the amino acid histidine in a minimal bacterial culture medium. In the presence of mutagenic chemicals, the defective gene may be mutated back to the functional state that allows the bacterium to grow in the medium. Because positive findings in the *Salmonella* reverse mutation assay have a good correlation with the outcome of rodent carcinogenicity testing, a positive result can trigger the discontinuation of further development, particularly for drug candidates intended for non-life-threatening indications.

Reactive metabolite trapping studies have proven useful in elucidating mutagenic mechanisms of drug candidates, and the mechanistic insights gathered have been used in the rational design of follow-on compounds that are devoid of genotoxic response. An example is evident with the 5-hydroxytryptamine 2C agonist and anti-obesity agent **67** (Fig. 20), which was mutagenic in the bacterial *Salmonella* Ames assay in an Aroclor 1254-induced rat liver S-9/NADPH-dependent fashion.[68,69] In the *Salmonella* assay, **67** produced a significant increase of mutations only in strains TA100 and TA1537 that are known to be sensitive to mainly base-pair and frame-shift mutagens, consistent with covalent adduction to DNA (rather than a simple intercalation). Studies with [^{14}C]-**67** revealed the

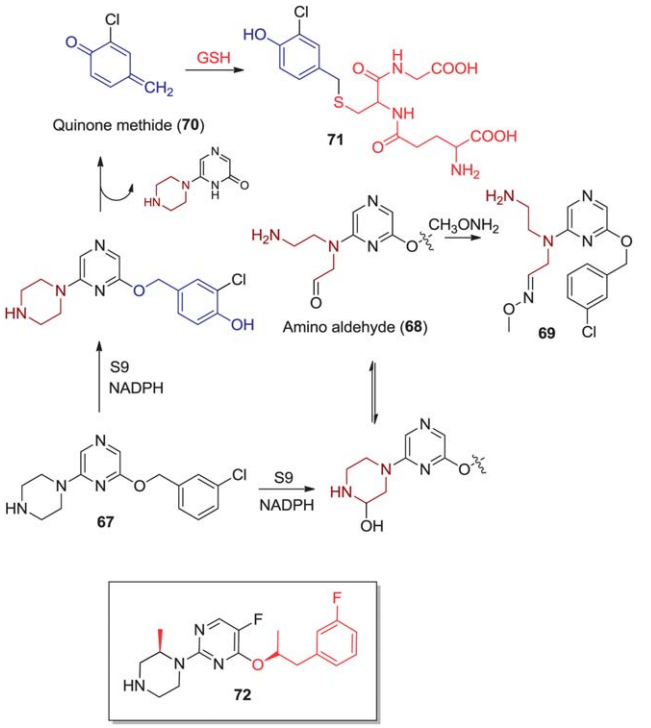

Fig. 20 Insights into the S9/NADPH-dependent mutagenic response with the 5-hydroxytryptamine 2C agonist **67** that led to the design of non-mutagenic analog and clinical candidate **72**.

irreversible and concentration-dependent incorporation of radioactivity in calf thymus DNA in an S-9/NADPH-dependent fashion, confirming that **67** was metabolized to a DNA-reactive metabolite. Reactive metabolite trapping studies in S-9/NADPH incubations led to the detection of GSH and amine conjugates. Structural elucidation of these conjugates allowed an insight into the mechanism leading to the formation of DNA-reactive metabolites (Fig. 20). The mass spectrum of the methoxylamine conjugate of **67** (*i.e.*, compound **69**) was consistent with condensation of amine with an electrophilic, aldehyde metabolite **68** derived from piperazine ring scission in **67**, whereas the mass spectrum of the GSH conjugate **71** suggested a bioactivation pathway involving initial aromatic ring hydroxylation on the 3-chlorobenzyl motif in **67** followed by β-elimination to an electrophilic quinone-methide species **70** that reacted with GSH. The observation that methoxylamine and GSH reduced mutagenic response in the Ames test suggested that the trapping agents competed with a DNA base(s) towards covalent adduction with the reactive metabolites. Overall, the exercise provided indirect information on the structure of DNA-reactive intermediates leading to mutagenic response with **67** and hence a rationale on which to base subsequent chemical intervention strategy for designing non-mutagenic back-up 5-hydroxytryptamine 2C agonists such as compound **72** (Fig. 20).[69] In contrast with **67**, **72** cannot form the reactive quinone methide species. Likewise, introduction of the methyl group is thought to shunt metabolism from piperazine ring opening to hydroxylation of the methyl substituent. Based on additional preclinical and safety profiling, compound **72** was nominated as a clinical candidate. Additional illustrations of drug design strategies to eliminate DNA-reactive metabolite formation have also appeared in the chemical toxicology literature.[70,71]

4.2 Eliminating mechanism-based inactivation of CYP enzymes

Modulation of CYP activity *via* induction or inhibition by xenobiotics including drugs can lead to clinical DDIs with consequences ranging from loss of efficacy to the introduction of adverse effects, respectively, for co-administered "victim" drugs. DDIs arising from CYP inhibition are more frequent and, in some cases, have resulted in the withdrawal of the marketed "perpetrator" drug (*e.g.*, the antihypertensive agent mibefradil), especially when these agents are associated with potent inhibition of CYP3A4. CYP inhibitors can be categorized as reversible (competitive or non-competitive), quasi-irreversible and irreversible in nature.[64]

Reversible inhibition usually involves two or more agents competing for metabolism at the active site of a CYP isozyme, with one drug inhibiting the metabolism of the other agent. In contrast, drugs converted to reactive metabolites by CYP may interact with the CYP quasi-irreversibly or irreversibly leading to enzyme destruction. Quasi-irreversible inactivation occurs when the reactive species complexes with the ferrous form of heme (a product of the reduction of the resting state ferric enzyme by NADPH-CYP reductase) in a strong, non-covalent interaction referred to as a metabolite intermediate (MI) complex. CYP inactivation can also arise through covalent adduction of the reactive metabolite to the heme prosthetic group and/or to an active site amino acid residue in the apoprotein. As such, CYP isozymes inactivated *via* these mechanisms are rendered catalytically incompetent, and must be replenished by newly synthesized protein. The phenomenon is oftentimes referred to as time-dependent inactivation (TDI), mechanism-based inactivation (MBI), and/or suicide inactivation.

By definition, time-dependent enzyme inhibitors are compounds that display an increasing degree of CYP inhibition upon increased duration of pre-incubation with the enzyme in a NADPH-dependent fashion (often consistent with metabolism to a reactive metabolite). The important kinetic constants for assessing the potential severity of CYP inactivation include the maximal inactivation rate constant (k_{inact}), inactivator concentration that yields half of the maximum inactivation rate (K_I), and the partition coefficient. From a drug discovery standpoint, large k_{inact} and small K_I values generally increase the likelihood of DDIs resulting from CYP inactivation. In preclinical drug discovery, the efficiency of CYP inactivation within a given chemical series can be gauged from the k_{inact}/K_I ratio. The partition coefficient is a measure of inactivation efficiency, and also can be a useful parameter to obtain for rank-ordering CYP inactivators. Mechanism-based inactivators are substrates of the enzymes they inactivate. The partition coefficient represents the ratio of the number of inactivator molecules that get metabolized relative to the number of enzyme molecules inactivated.

In vitro experimental protocols to measure k_{inact} and K_I for major human CYP enzymes are labour-intensive and are generally not amenable to high-throughput screening in early drug discovery programs. As a result, methodologies for quantitative assessment of CYP MBI without the need for generating K_I and k_{inact} values have been described, and these enable the assessment and/or elimination of the DDI risk (arising from CYP inactivation) prior to candidate selection. The "scaled-down" methods typically are used to detect: (a) time-dependent loss of CYP activity following incubation at a single compound concentration and/or (b) a shift in the IC_{50} following pre-incubation at multiple concentrations of the compound of interest.[65]

Compared to reversible CYP inhibition, drug-induced time-dependent inactivation of CYPs presents a greater safety concern because of the increased propensity for pharmacokinetic interactions upon multiple dosing and the sustained duration of these interactions after discontinuation of the mechanism-based inactivator. Furthermore, depending upon the fraction of the mechanism-based inactivator that is metabolized by the inactivated CYP, an additional clinical consequence could involve supraproportional increases in systemic exposure of the inactivator itself after multiple doses. Finally, covalent modification of CYP enzymes can also lead to hapten formation and can, in some cases, trigger an autoimmune response in susceptible patients leading to idiosyncratic toxicity.[64]

In theory, MBI of CYP enzymes can be caused by any molecule that is bioactivated to a reactive metabolite by a CYP isoform. However, in reality, not all reactive metabolite-positive compounds will covalently modify CYPs. In many such cases, the reactive species will escape from the active site into solution prior to the inactivation step. Upon release from the CYP active site, the reactive metabolites do, however, have the potential to react non-specifically with other macromolecules and/or DNA. The reactive metabolite can be detoxified (*via* reaction with GSH) or covalently adduct to cellular proteins, potentially resulting in some form of immune-mediated idiosyncratic toxicity.[65]

A pragmatic starting point to deal with CYP TDI in early discovery should involve mechanistic studies to elucidate the biochemical/molecular basis for enzyme inactivation, followed by rational structural manipulations and iterative SAR analysis for time-dependent CYP inactivation. Hopefully, this will result in the identification of structural types wherein the TDI liability has been eliminated or drastically reduced, relative to the prototype(s). Such an approach serves a dual purpose of abolishing CYP inactivation liability as well as eliminating the potential for formation of protein-reactive metabolites that may potentially lead to idiosyncratic toxicity. It is noteworthy to point out that prior to embarking on a laborious exercise to dial out CYP inactivation and/or reactive metabolite formation, insights into the anticipated human pharmacokinetics and the daily dosing regimen for a CYP mechanism based inactivator and reactive metabolite-positive compound are essential. For example, the estrogenic contraceptive ethinyl estradiol is metabolised by CYP3A4 at the C-17α terminal alkyne motif to a

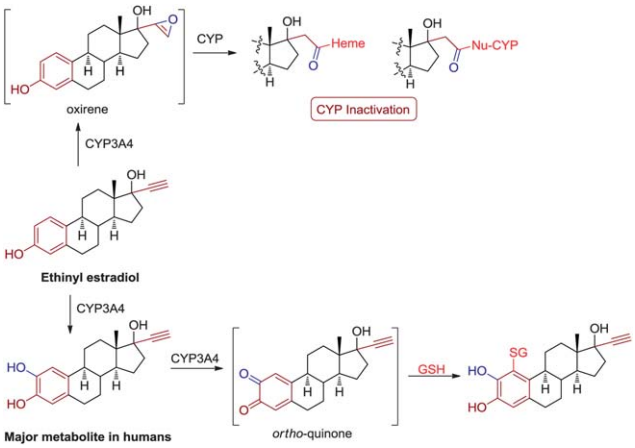

Fig. 21 Bioactivation of ethinyl estradiol into CYP3A4- and protein-reactive metabolites.

reactive oxirene species, which alkylates the heme group and/or protein resulting in the MBI of the isozyme (Fig. 21).[72,73] In addition to acetylene bioactivation, Park *et al.*[74] have demonstrated the oxidation of the phenol ring in ethinyl estradiol to an electrophilic *ortho*-quinone species (*via* the intermediate catechol metabolite) in HLM, a process that eventually leads to microsomal covalent binding, a potential marker of idiosyncratic hepatotoxicity.[75] The lack of DDI with CYP3A4 substrates and/or idiosyncratic toxicity due to reactive metabolite formation is most likely due to the very low daily dose of 0.035 mg (which results in systemic concentrations far below the threshold required to inactivate CYP3A4 activity *in vivo*) of ethinyl estradiol that is used in birth control.

In cases where the functional group(s) responsible for CYP inactivation is required for primary pharmacology, some companies will choose an advance CYP mechanism-based inactivator as a clinical candidate, especially if there is reason to believe that the combination of *in vivo* systemic exposure needed for efficacy relative to the potency of CYP inactivation will not result in a clinically relevant DDI. In the latter case, confidence in the ability to predict clinical DDI from *in vitro* DDI data becomes a critical component in the decision to advance an *in vitro* CYP inactivator into the clinic. Although much progress has been made in DDI prediction capabilities, there exists uncertainty in several of the input parameters (in particular predicted human pharmacokinetics and degradation rates of CYP) that are used to generate the prediction in early discovery, and hence over- or underprediction of DDI is not uncommon.[64]

Recently, several publications have demonstrated tactics to minimize and/or eliminate time-dependent inactivation of CYP enzymes without affecting primary pharmacology and/or disposition characteristics. Solutions range from modulation of lipophilicity resulting in diminished rates of metabolism (and bioactivation to reactive metabolites) to virtually eliminating the potential for reactive metabolite formation *via* blocking the site of bioactivation and/or removal of the structural alert. Alterations in physicochemical properties within

mechanism-based inactivators will diminish rates of enzyme inactivation but may not completely eliminate the liability.

Reduction of CYP3A4 inactivation *via* a lowering of lipophilicity was successfully applied by Westaway and coworkers in their work, leading to the discovery of the first small molecule agonist of the motilin receptor (Fig. 22).[76] The lead compound **73** revealed CYP3A4 inhibition in HLM (~14–fold decrease in IC_{50} upon preincubation for 30 min; IC_{50} at 0–5 min = 20 μM; IC_{50} at 25–30 min = 1.4 μM) in a manner consistent with time-dependent inactivation. Based on the hypothesis that the CYP interaction is driven by size and lipophilicity, analogues of **73** were designed with reduced molecular weight and *c*log *P*. Thus, replacement of the pyridyl and dimethylpiperazine rings of **73** with a two-carbon linker and (2*S*)-methylpiperazine ring, respectively, led to compounds with reduced agonist potency; however, these changes in combination with a terminal 3-fluoro substituent afforded **74**, which demonstrated an improved CYP3A4 inhibition profile (<3.2-fold decrease in CYP3A4 IC_{50} in a 30 min preincubation; IC_{50} at 0–5 min = 10 μM; IC_{50} at 25–30 min = 3.1 μM) compared to **73**, while retaining motilin potency. Further reduction in the linker size afforded **75**, which demonstrated a notable improvement in agonist potency and preclinical pharmacokinetics (relative to **73**) and drastically attenuated CYP inactivation (<2-fold decrease in CYP3A4 IC_{50} in a 30 min preincubation; IC_{50} at 0–5 min = 26 μM; IC_{50} at 25–30 min = 18 μM).

Another example of utilizing lipophilicity modulation to reduce time-dependent inactivation of CYP enzymes is evident with the 4,4-disubstituted piperidine series as glycine transporter 1 (GlyT1) inhibitors for potential treatment of schizophrenia.[77] Replacing the C-4 phenyl group in the lead piperidine derivative **76**, a time-dependent CYP inactivator, with the 2-pyridyl group, removing the metabolically labile chiral methyl and aniline NH_2 groups led to a net reduction in log *P* by 0.6 log units and abrogated CYP inactivation potential in the resulting compound **77** (Fig. 22). An additional 0.8 log unit reduction in lipophilicity was achieved by replacing one of the aromatic chlorine atoms with two fluorine atoms leading to **78**, which was virtually devoid of CYP inactivation liabilities. Compound **78** also displayed improvements in aqueous solubility and exhibited GlyT1 potency comparable to **76**.

Elimination of CYP MBI caused by covalent modification by reactive metabolite can also be achieved by replacing the structural motif prone to bioactivation with a metabolically latent functional group or *via* strategic placement of a complementary substituent(s) to block the site of initial metabolism that precludes the formation of reactive species. PF-562271 (**79**) (Fig. 23) is a dual inhibitor of the focal adhesion kinase and proline-rich tyrosine kinase 2 with potential utility in the treatment of ovarian cancer and osteoporosis.[78] *In vitro* metabolism studies in HLM revealed that **79** is a CYP3A4 substrate and a time-dependent inactivator suggesting that the agent could inhibit its own clearance mechanism *in vivo*. The mechanism of CYP3A4 inactivation was shown to occur *via* a

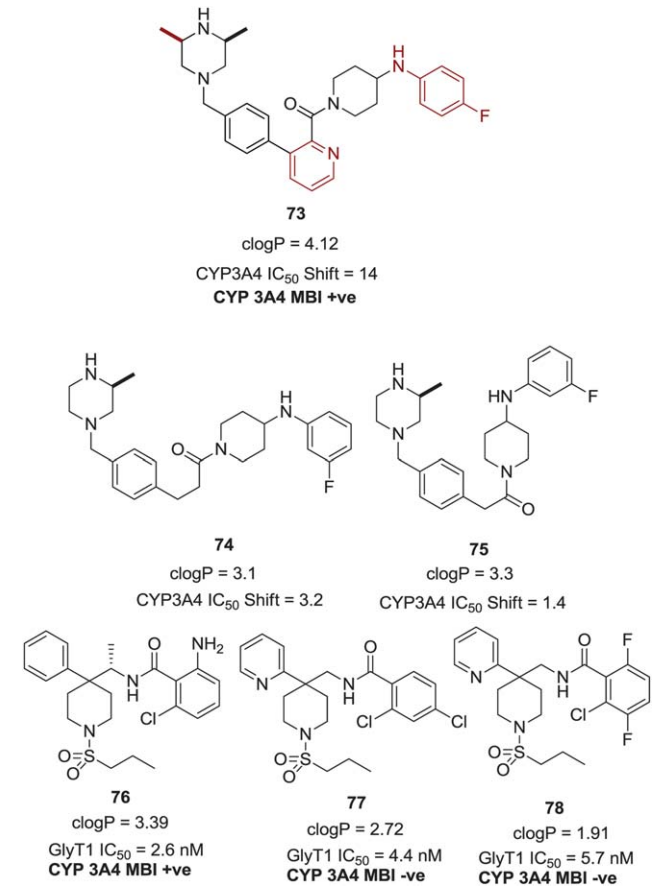

Fig. 22 Manipulations of physicochemical properties to attenuate time-dependent inactivation of CYP enzymes.

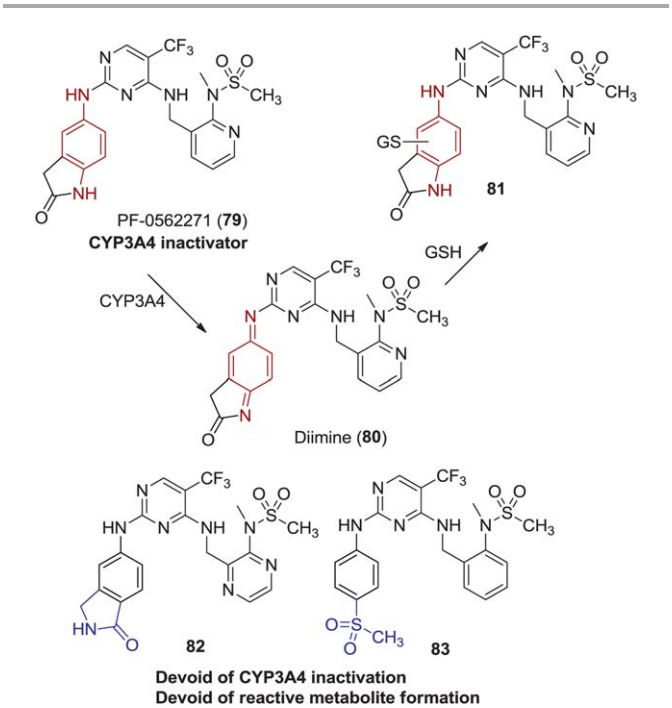

Fig. 23 Strategies to eliminate CYP3A4 time-dependent inactivation by virtue of eliminating reactive diimine formation with oxindole-based focal adhesion kinase inhibitors.

two-electron oxidation of the dianiline motif to a reactive diimine species **80**, which was trapped with GSH to yield adduct **81** (Fig. 23).[79] Furthermore, **79** demonstrated supraproportional increases in oral systemic exposure upon repeated dosing in clinical trials, a phenomenon that was consistent with self-inactivation of its clearance mechanism (unpublished Pfizer data on file). Likewise, **79** also caused a greater than three-fold increase in the systemic exposure of the probe CYP3A4 substrate midazolam in a clinical DDI study. Insights into the mechanism of CYP3A4 inactivation allowed a rational medicinal chemistry strategy to reduce/eliminate enzyme inactivation liability.[79] Thus, simply exchanging the 5-aminooxindole nitrogen and carbonyl groups in the parent compound or removing the bis-aniline framework altogether afforded analogs (*e.g.*, **82** and **83**) that were virtually devoid of CYP3A4 inactivation, while maintaining kinase potency. In general, disruption of the electron-rich dianiline structure present in **79** also mitigated potential IADR risks in the course of SAR studies.[79]

Paroxetine (**84**) (Fig. 24) is a selective serotonin reuptake inhibitor that inhibits CYP2D6 in a time- and concentration-dependent fashion consistent with MBI.[80] MBI of CYP2D6 by paroxetine occurs during metabolism of the 1,3-benzdioxole ring. Thus, hydrogen atom abstraction from the methylene carbon followed by elimination of water from a hydroxymethylene intermediate generates a carbene intermediate, which forms a MI complex with the ferrous form of the heme iron atom in CYP2D6 resulting in a catalytically inactive enzyme (Fig. 24).[81] Because CYP2D6 is responsible for paroxetine metabolism, MBI of CYP2D6 activity by paroxetine is associated with non-linear pharmacokinetics in CYP2D6 extensive metabolizers.[82] Likewise, DDIs with co-administered drugs whose clearance is mediated by CYP2D6 have been demonstrated.[83–85] Against this backdrop, *in vitro* metabolism studies with the doubly deuterated paroxetine analogue CTP-347 (**85**) (Fig. 24) demonstrated little to no time-dependent inactivation of CYP2D6, apparently due to a dramatic reduction in the formation of the reactive carbene intermediate.[86] Compound **85** is currently in clinical trials for the treatment of hot flashes in menopausal women, and has been studied in a 96-patient single- and multiple-ascending dose clinical trial. The multiple-dose subjects initially received a single dose of dextromethorphan (a probe CYP2D6 substrate), followed by 14 days of treatment with **85**, then another single dose of dextromethorphan. Subjects receiving **85** at 20–40 mg once-a-day (QD) retained a substantially greater ability to metabolize dextromethorphan compared to treatment with paroxetine administered at 20 mg QD (~15 to 20% inhibition of CYP2D6-catalyzed dextromethorphan metabolism to dextrorphan *vs.* ~55 to 60% inhibition of CYP2D6 activity with paroxetine). As such, this clinical DDI represents the first clinical demonstration that deuteration can be utilized to ameliorate DDI liabilities due to mechanism-based inactivation of CYP enzymes.

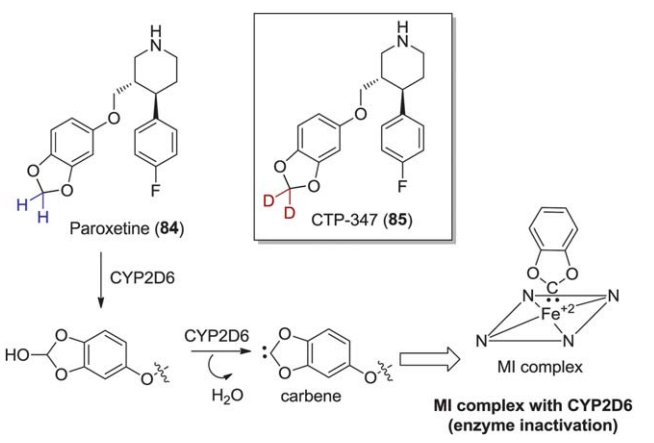

Fig. 24 Attenuating CYP mechanism-based inactivation liability through deuterium incorporation at the metabolically labile site as illustrated with the antidepressant paroxetine.

4.3 Mitigating risks of idiosyncratic toxicity *via* elimination of reactive metabolite formation

While the potential for genotoxicity and DDI can be examined directly from *in vitro* assays, the same does not often hold true for immune-mediated IADRs (*e.g.*, hepatotoxicity, skin rashes, agranulocytosis, and aplastic anemia) in drug-treated patients. IADRs are unrelated to known drug pharmacology, and occur at very low incidence (1 in 10 000 to 1 in 100 000). Consequently, these reactions are often not detected until the drug has gained broad exposure in a large patient population. An understanding of the biochemical basis for drug toxicity has replaced the vague perception of a chemical class effect with a sharper picture of individual molecular peculiarity. There are several instances of prototype drugs associated with IADRs that also form reactive metabolites; elimination of reactive metabolite liability in follow-on successor agent(s) markedly improves the safety profile.

Although the evidence is most often anecdotal in nature, a compelling case for chemotype-based toxicity can be inferred from such structure–toxicity analyses.[87] For instance, in the case of the nonsteroidal anti-inflammatory drug sudoxicam (**86**), hepatotoxicity observed in the clinic that led to its suspension in clinical trials has been attributed to thiazole ring scission yielding a reactive acylthiourea metabolite **87** capable of oxidizing GSH and proteins (Fig. 25).[88] The structurally related anti-inflammatory drug meloxicam (**88**) does not possess the hepatotoxic liability associated with sudoxicam. Although introduction of a methyl group at the C5 position on the thiazole ring in meloxicam is the only structural difference, the change dramatically alters the metabolic profile such that oxidation of the C5 methyl group to the alcohol metabolite **89** constitutes the principal metabolic fate of meloxicam in humans (Fig. 25).

Due to the inability to predict and quantify the risk of IADRs, and because reactive metabolites as opposed to the parent molecules from which they are derived are thought to be responsible for the pathogenesis of many IADRs, detection of a reactive metabolite(s) in the course of metabolism is considered to be an undesirable trait in preclinical drug discovery, particularly for high daily dose drug candidates intended to treat non-life threatening diseases.[65] Examples of medicinal chemistry

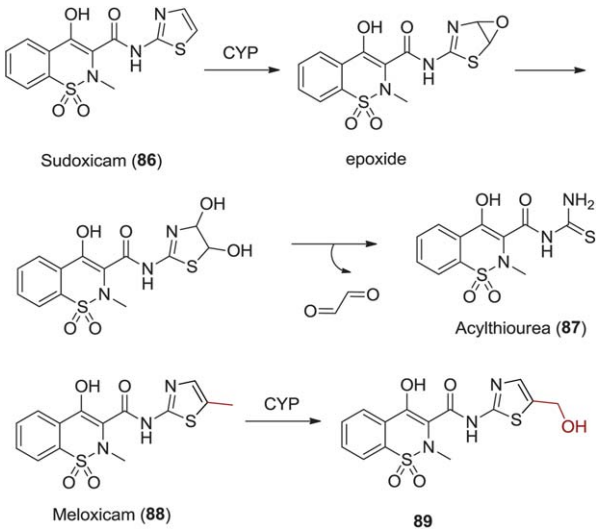

Fig. 25 Structure–toxicity relationships: the tale of the magic methyl.

tactics to eliminate reactive metabolite formation are abundant in the literature. For instance, in the course of discovery efforts leading to the discovery of taranabant (**91**) (Fig. 26), a selective and potent inhibitor of the cannabinoid-1 (CB-1) receptor, and a phase III clinical candidate for the treatment of obesity, lead compound **90** (Fig. 26) revealed a high level of covalent binding to HLM in a NADPH-dependent fashion, consistent with reactive metabolite formation. Elucidation of the structure of the GSH conjugate suggested that the reactive metabolite was an arene oxide intermediate derived from epoxidation of the electron rich phenoxy ring.[89] Replacement of the phenoxy ring with the trifluoromethylpyridyl ring afforded **91**, which was devoid of reactive metabolite formation, while retaining potency against the CB-1 receptor.

Another example pertains to the discovery of the first glucokinase activator, piragliatin (**92**) (Fig. 27), which has shown efficacy (*e.g.*, lowering of pre- and postprandial glucose levels, improvements in insulin secretory profile, *etc.*) in phase II clinical trials in patients with type 2 diabetes.[90] The prototype candidate RO0281675 (**93**) was withdrawn from phase I clinical studies due to its narrow safety margin in preclinical toxicology studies. Compound **93** caused reversible hepatic lipidosis in chronic toxicology studies in rats and dogs, which was believed to occur *via* the bioactivation of the 2-aminothiazole motif in **93**

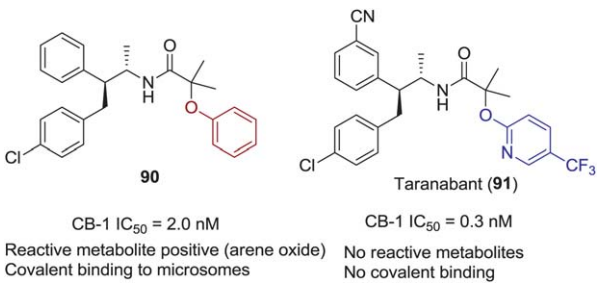

Fig. 26 Elimination of reactive metabolite liability in the discovery of taranabant, a selective and potent CB-1 receptor antagonist, and anti-obesity agent.

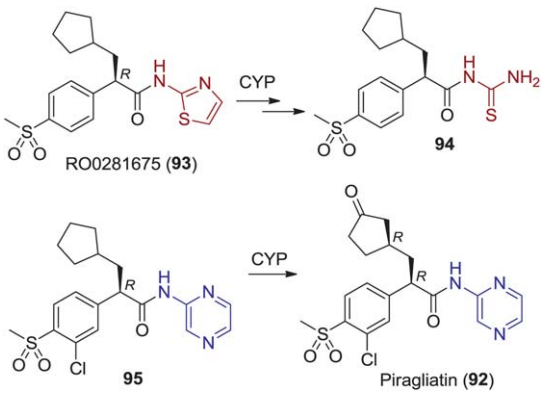

Fig. 27 Elimination of the reactive metabolite liability in the discovery of piragliatin, the first glucokinase activator, and anti-diabetic agent.

to a thiourea metabolite **94** (similar to the situation depicted with the anti-inflammatory drug sudoxicam in Fig. 25). The hypothesis was further substantiated on the basis of two observations: (a) thiourea **94** was formed as a metabolite upon incubating **93** in NADPH-supplemented liver microsomes from preclinical species and humans, and (b) five day toxicity studies in rats with an authentic standard of **94** led to hepatic lipidosis in a manner similar to that noted with **93**. Attempts to identify a 4,5-disubstituted or 4- or 5-monosubstituted thiazole derivative of **93** that would be devoid of thiourea formation, while maintaining glucokinase activation potency and adequate ADME properties, were unsuccessful. However, subsequent SAR studies seeking thiazole ring replacements led to the identification of a pyrazine-based lead analogue **95**. *In vitro* metabolite identification on **95** revealed several oxidative metabolites on the cyclopentyl ring, which were subsequently shown to possess pharmacological activity comparable to **93**. Additional profiling of *in vitro* and *in vivo* safety and efficacy of the oxidative metabolites led to the selection of **92** as the clinical candidate. Subchronic and chronic toxicology studies with **92** in rats and dogs revealed no evidence of hepatic lipidosis. Furthermore, **93** is relatively less lipophilic than **92** (*clog P* of **92** = 2.69 *vs. clog P* of **93** = 0.47) and exhibits superior oral absorption (lower CL leading to increased oral *F*) in preclinical species and humans.

In the Pfizer glucokinase activator program, a unique metabolic liability of the 4-sulfonyl-2-pyridone ring system was encountered in the lead compound **96** (Fig. 28).[91,92] The heterocyclic ring system readily underwent conjugation with GSH under non-enzymatic (pH 7.4 phosphate buffer) as well as enzyme-catalyzed (HLM, human liver cytosol and human glutathione transferases) conditions in a near quantitative fashion to yield adduct **97**.[91] The identification of **97** in circulation following intravenous administration of **96** to rats confirmed the relevance of the *in vitro* findings.[92] The observation that **96** was intrinsically electrophilic was alarming, considering the potential for indiscriminate alkylation of proteins and DNA in a fashion similar to alkyl halides and Michael acceptors, which are generally associated with toxicity. Consequently, further investment in the 4-sulfonyl-2-pyridone class of compounds was suspended, and instead efforts were

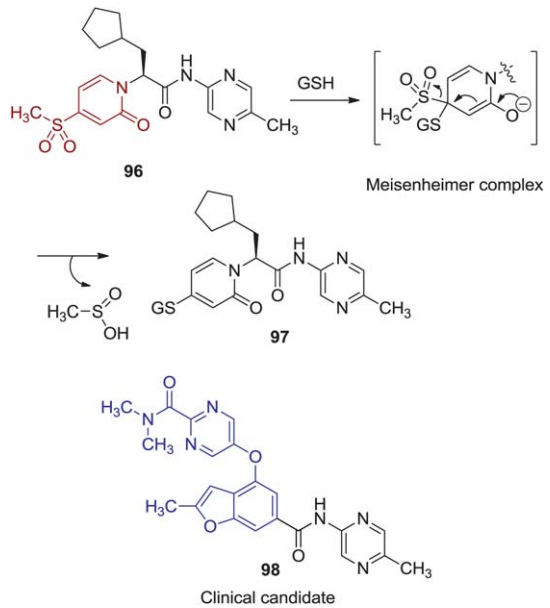

Fig. 28 Identification of innately electrophilic lead chemical matter in a series of glucokinase activators.

initiated on the optimization of a series of benzofuran-aminopyrimidine derivatives, from which emerged the clinical candidate **98** (see Fig. 28), which is currently in phase II clinical trials for the treatment of type 2 diabetes.[93]

A final example, which focuses on eliminating reactive metabolite liability within a lead chemical series, is evident with the 2-anilino-7-aryl-pyrrolo[2,1-*f*][1,2,4]triazine class of anaplastic lymphoma kinase (ALK) inhibitors.[94,95] The lead compound **99** (Fig. 29) was orally efficacious in ALK-dependent tumor xenografts in mice; however, examination of reactive metabolite formation in HLM revealed extensive CYP-mediated oxidation of the *p*-dianiline moiety to a reactive quinone-dimine **100**, which was trapped with GSH to afford adduct **101**.[95] The magnitude of bioactivation (as judged from the semi-quantitation of the GSH adducts) in this subset of pyrrolotriazines was quite unexpected when compared to the much lower levels listed in the literature for drugs associated with IADRs.[95] To mitigate the reactive metabolite liability, a three-pronged strategy was adopted (Fig. 30): (a) installation of electron withdrawing substituents to the site of oxidation, (b) shifting the position of the saturated heterocycle on the aniline ring, and (c) modifying the heterocycle to remove the *p*-nitrogen of the ring.

Introduction of small electron withdrawing groups at the C2 (*e.g.*, compound **102**) or even the C4 position resulted in ~80% reduction in GSH adduct formation relative to **99**. However, fluorination was also accompanied by the loss of activity in ALK

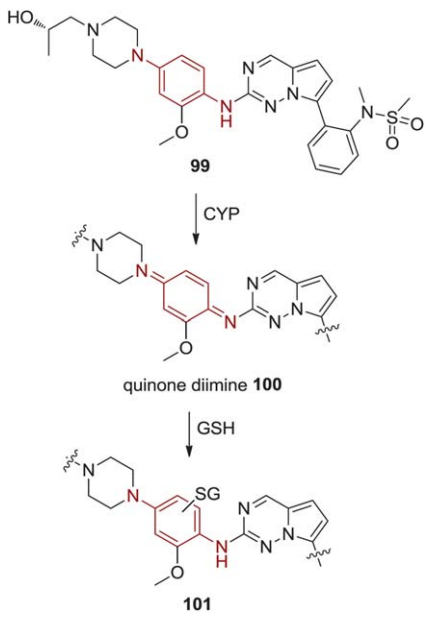

Fig. 29 Bioactivation of 2-anilino-7-aryl-pyrrolo[2,1-*f*][1,2,4]triazine class of ALK inhibitors.

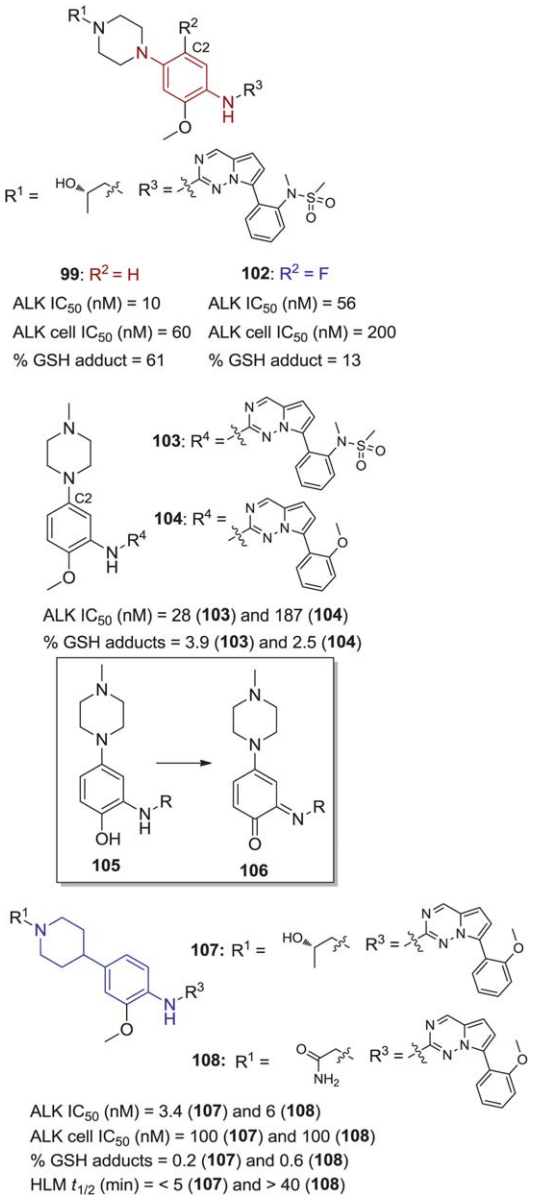

Fig. 30 Elimination of the reactive metabolite liability in ALK inhibitor **99**.

enzyme and cell-based primary assays. Shifting the piperazine ring from the *para* to the *meta* position of the aniline ring (*e.g.*, compounds **103** and **104**) eroded pharmacologic potency, and also led to the formation of a reactive *o*-iminoquinone **106** (instead of the *p*-diiminoquinone species) *via* a bioactivation pathway involving demethylation of the *O*-methoxy unit followed by two-electron oxidation of the 2-hydroxyaniline metabolite (**105**). Another approach to mitigate bioactivation involved replacement of the piperazine ring with a piperidine ring (*e.g.*, compound **107**). In this scenario, the oxidation potential of the *p*-CH-anilines was expected to be dramatically diminished relative to the dianilines, which mitigated the prospect of quinone-methide formation. Compound **107** validated this strategy, generating trace levels of GSH adduct, *via* demethylation and bioactivation to the *o*-iminoquinone species with no formation of imino-quinone-methide detected. This very low level of GSH adduct was considered acceptable to pursue this strategy further, and led to the optimized and orally bioavailable candidate **108** with significant human liver microsomal stability over **107**.

5 Characterization of active metabolites

In most cases, the biotransformation of drugs leads to the formation of pharmacologically inactive metabolites. However, there are instances where drug metabolism can result in the formation of active metabolites.[96] The generation of active metabolites can be mediated by both phase I (oxidation, reduction and hydrolysis) and phase II (glucuronidation and sulphation) metabolism. In some scenarios, metabolite formation may be crucial for the pharmacological activity associated with the parent molecule. For instance, minoxidil (**109**) sulfation in keratinocytes to the sulfate conjugate (**110**) (Fig. 31) is the rate-limiting step in stimulation of hair growth upon administration of minoxidil.[97] Likewise, oxidative ring scission of the thiophene ring in clopidogrel (**111**) by CYP2C19 generates thiol metabolite (**112**) (Fig. 31), which forms a covalent disulfide adduct with the P_2Y_{12} receptor in platelets, and leads to the beneficial inhibitory effects on platelet aggregation.[98,99] Furthermore, active metabolites can possess superior pharmacologic, pharmacokinetic and safety profiles compared to their respective parent compounds. Illustrations wherein active metabolites have been developed as drugs (or drug candidates) with improved profiles relative to the precursor drug are plentiful. A classic example is that of the antihistamine agent fexofenadine (**114**), the active metabolite of terfenadine (**113**) (Fig. 32).[100] Terfenadine undergoes extensive first-pass metabolism that is predominantly mediated by CYP3A4, and forms fexofenadine as the major circulating metabolite (see Fig. 32).[101] Terfenadine itself is now known to be a potassium channel inhibitor, leading to QT interval prolongation, such that co-administration of terfenadine with CYP3A4 inhibitors is known to result in potentially fatal cardiac arrhythmias.[102] In contrast, no change in QT interval was observed with fexofenadine when administered alone or in combination with the CYP3A4 inhibitor ketoconazole. As a result, when terfenadine was withdrawn from the market, it was possible to replace it with fexofenadine. Likewise, marketed drugs desloratadine (**116**) and desvenlafaxine (**118**) are active metabolites of the first-generation agents loratadine (**115**) and venlafaxine (**117**), respectively.[103,104]

An excellent example of drug design *via* an understanding of the bioactivity profile of drug metabolites becomes evident with the cholesterol absorption inhibitor ezetimibe (**124**) (Fig. 33).[105] Discovery efforts that ultimately led to ezetimibe initially began

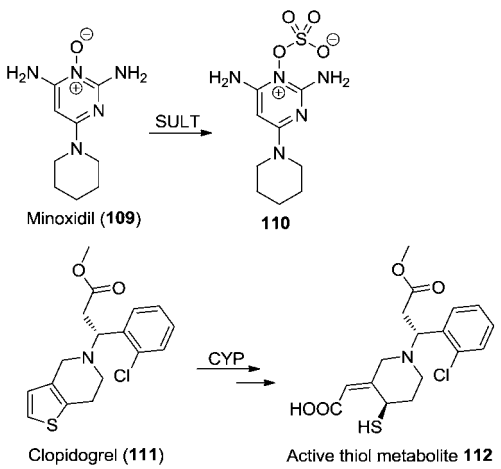

Fig. 31 Formation of active metabolites responsible for pharmacology for the parent drug.

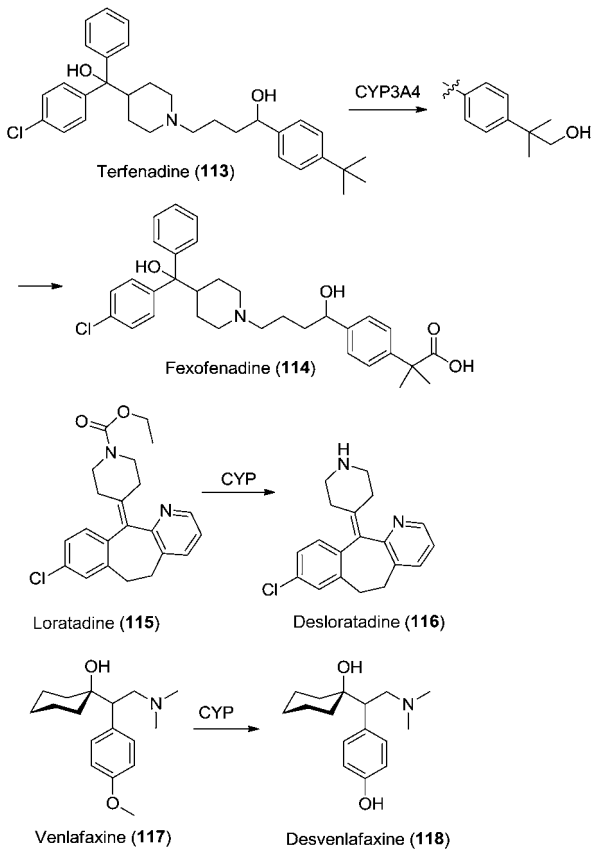

Fig. 32 Some examples of active metabolites that have been developed and marketed as drugs.

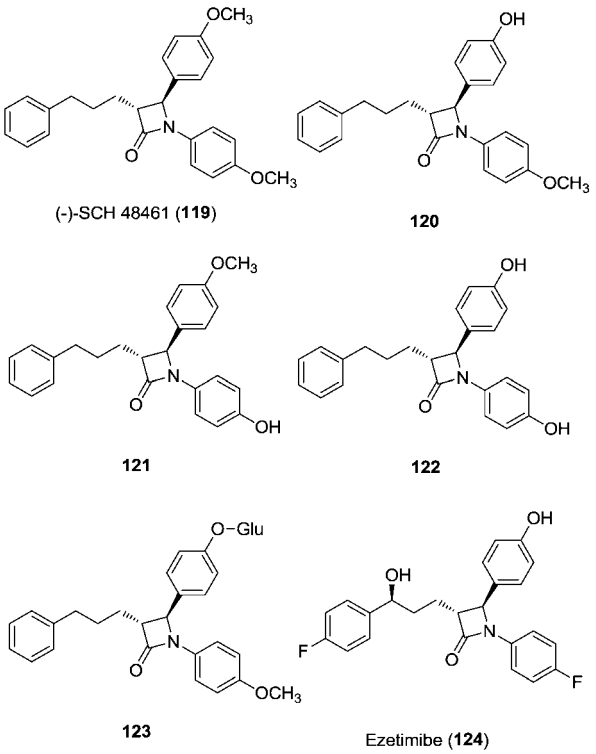

Fig. 33 Discovery of the cholesterol lowering agent ezetimibe (**124**) through bioactivity profiling of metabolites.

as a program to discover novel inhibitors of acyl coenzyme A cholesterol acyltransferase (ACAT) using rodent animal models as a pharmacology screen (in the absence of relevant *in vitro* assays to rank order intrinsic potency). An interesting finding in this effort was the robust reduction of serum cholesterol and blockade of hepatic cholesterol accumulation by certain azetidinone derivatives (*e.g.*, (−)-SCH48461, **119**), which had virtually no inhibitory activity against ACAT. A substantial part of the discovery effort was next devoted to the understanding of the molecular target of **119**, which was further confounded by the fact that **119** is extensively metabolized *in vivo*, making it unclear as to what the active species is. Bioactivity profiling using bile from animals dosed with [^{14}C]-**119** led to the characterization of several active metabolites of **119**, which included phenols (compounds **120–122**) derived from the mono- and bis-*O*-demethylation and even a glucuronide conjugate (**123**). The *in vivo* potency of these metabolites determined further SAR optimization. As such, when one examines the structure of ezetimibe (**124**), it is clear that the introduction of two fluorine atoms in **120** was a critical step towards increased resistance to metabolism, while maintaining potent reduction in cholesterol levels.

6 Concluding remarks

It is clear from our own experience and from the general literature that metabolism-guided drug design has been readily embraced by the pharmaceutical industry as an approach to mitigate attrition due to poor pharmacokinetics. From an ADME perspective, the major utility of metabolism studies in drug discovery lies in the identification of relevant clearance mechanisms for lead chemical matter, which then helps to choose the most relevant *in vitro*/*in vivo* models for making high confidence projections of human pharmacokinetics prior to first-in-human testing. From a medicinal chemistry perspective, the value lies in the identification of a suboptimal metabolic profile at the molecular level, and in the subsequent ability to derive a logical hypothesis on how to address metabolism-related issues. As such, elucidation of metabolic pathways of new drug candidates in preclinical species of toxicology and humans is pivotal in the characterisation of disproportionate or human-unique metabolites, especially in the light of regulatory guidance pertaining to metabolites in safety testing (MIST).[106–108] Recently, many efforts have been made to understand reactive metabolite liabilities and although the link between metabolism and IADRs remains elusive, it remains prudent to continue to explore these relationships as early as possible in drug development, if for no other reason than to give medicinal chemists the option of pursuing an alternate chemical series devoid of such concerns. Finally, as novel (and proprietary) functional groups are continuously sought in drug design, drug metabolism scientists will undoubtedly identify unanticipated bioactivation pathways leading to reactive metabolites, and *de novo* medicinal chemistry strategies will be put into place to encounter the liability. Certainly, a scan of the medicinal chemistry literature indicates numerous illustrations of such phenomena and, in particular, the invaluable marriage of medicinal chemistry/drug metabolism groups in providing prospective solutions to such problems.[109–113]

Notes and references

1 H. van de Waterbeemd, D. A. Smith, K. Beaumont and D. Walker, *J. Med. Chem.*, 2001, **44**, 1313–1333.
2 I. Kola and J. Landis, *Nat. Rev. Drug Discovery*, 2004, **3**, 711–715.
3 R. J. Riley, *Curr. Opin. Drug Discovery Dev.*, 2001, **4**, 45–54.
4 J. A. Williams, R. Hyland, B. C. Jones, D. A. Smith, S. Hurst, T. C. Goosen, V. Peterkin, J. R. Koup and S. E. Ball, *Drug Metab. Dispos.*, 2004, **32**, 1201–1208.
5 R. S. Obach, *Drug Metab. Dispos.*, 1999, **27**, 1350–1359.
6 Y.-Z. Shu, B. M. Johnson and T. J. Yang, *AAPS J.*, 2008, **10**, 178–192.
7 M. Strolin-Benedetti, R. Whomsley and E. Baltes, *Expert Opin. Drug Metab. Toxicol.*, 2006, **2**, 895–921.
8 D. C. Pryde, D. Dalvie, Q. Hu, P. Jones, R. S. Obach and T. D. Tran, *J. Med. Chem.*, 2010, **53**, 8441–8460.
9 A. S. Kalgutkar, D. K. Dalvie, N. Castagnoli, Jr and T. J. Taylor, *Chem. Res. Toxicol.*, 2001, **14**, 1139–1162.
10 N. A. Meanwell, *J. Med. Chem.*, 2011, **54**, 2529–2591.
11 D. A. Smith, E. Schmid and B. Jones, *Clin. Pharmacokinet.*, 2002, **41**, 1005–1019.
12 A. Wood and D. Armour, *Prog. Med. Chem.*, 2005, **43**, 239–271.

13 P. A. Williams, J. Cosme, D. M. Vinkovic, A. Ward, H. C. Angove, P. J. Day, C. Vonrhein, I. J. Tickle and H. Jhoti, *Science*, 2004, **305**, 683–686.
14 M. Ekroos and T. Sjögren, *Proc. Natl. Acad. Sci. U. S. A.*, 2006, **103**, 13682–13687.
15 J. K. Yano, M. R. Wester, G. A. Schoch, K. J. Griffin, C. D. Stout and E. F. Johnson, *J. Biol. Chem.*, 2004, **279**, 38091–38094.
16 H. Z. Bu, *Curr. Drug Metab.*, 2006, **7**, 231–249.
17 D. F. V. Lewis, M. N. Jacobs and M. Dickins, *Drug Discovery Today*, 2004, **9**, 530–537.
18 D. F. V. Lewis and M. Dickins, *Drug Discovery Today*, 2002, **7**, 918–925.
19 C. A. Lipinski, F. Lombardo, B. W. Dominy and P. J. Feeney, *Adv. Drug Delivery Rev.*, 2001, **46**, 3–26.
20 C. A. Bergstrom, M. Strafford, L. Lazorova, A. Avdeef, K. Luthman and P. Artusson, *J. Med. Chem.*, 2003, **46**, 558–570.
21 T. T. Wager, R. Y. Chandrasekaran, X. Hou, M. D. Troutman, P. R. Verhoest, A. Villalobos and Y. Will, *ACS Chem. Neurosci.*, 2010, **1**, 420–434.
22 A. F. Stepan, K. Karki, W. S. McDonald, P. H. Dorff, J. K. Dutra, K. J. Dirico, A. Won, C. Subramanyam, I. V. Efremov, C. J. O'Donnell, C. E. Nolan, S. L. Becker, L. R. Pustilnik, B. Sneed, H. Sun, Y. Lu, A. E. Robshaw, D. Riddell, T. J. O'Sullivan, E. Sibley, S. Capetta, K. Atchison, A. J. Hallgren, E. Miller, A. Wood and R. S. Obach, *J. Med. Chem.*, 2011, **54**, 7772–7783.
23 G. Wuitschik, E. M. Carreira, B. Wagner, H. Fischer, I. Parrilla, F. Schuler, M. Roger-Evans and K. Müller, *J. Med. Chem.*, 2010, **53**, 3227–3246.
24 C. M. Adams, C. W. Hu, A. Y. Jeng, R. Karki, G. Ksander, D. Lasala, J. Leung-Chu, G. Liang, Q. Liu, E. Meredith, C. Rao, D. F. Rigel, J. Shi, S. Smith, C. Springer and C. Zhang, *Bioorg. Med. Chem. Lett.*, 2010, **20**, 4324–4327.
25 Z. K. Wan, E. Chenail, J. Xiang, H. Q. Li, M. Ipek, J. Bard, K. Svenson, T. S. Mansour, X. Xu, X. Tian, V. Suri, S. Hahm, Y. Xing, C. E. Johnson, X. Li, A. Qadri, D. Panza, M. Perreault, J. F. Tobin and E. Saiah, *J. Med. Chem.*, 2009, **52**, 5449–5461.
26 Y. Cheng, F. Zhang, T. A. Rano, Z. Lu, W. A. Scheif, L. Gabryelski, D. B. Olsen, M. Stahlhut, C. A. Rutkowski, J. H. Lin, L. Jin, E. A. Emini, K. T. Chapman and J. R. Tata, *Bioorg. Med. Chem. Lett.*, 2002, **12**, 2419–2422.
27 D. M. Floyd, S. D. Kimball, J. Krapcho, J. Das, C. F. Turk, R. V. Moquin, M. W. Lago, K. J. Duff, V. G. Lee, R. E. White, R. E. Ridgewell, S. Moreland, R. J. Brittain, D. E. Normandin, S. A. Hedberg and G. C. Cucinotta, *J. Med. Chem.*, 1992, **35**, 756–772.
28 F. P. Guengerich, O. Okazaki, Y. Seto and T. L. Macdonald, *Xenobiotica*, 1995, **25**, 689–709.
29 A. Nagle, T. Wu, K. Kuhen, K. Gagaring, R. Borboa, C. Francek, Z. Chen, D. Plouffe, X. Lin, C. Caldwell, J. Ek, S. Skolnik, F. Liu, J. Wang, J. Chang, C. Li, B. Liu, T. Hollenbeck, T. Tuntland, J. Isbell, T. Chuan, P. B. Alper, C. Fischli, R. Brun, S. B. Lakshminarayana, M. Rottmann, T. T. Diagana, E. A. Winzeler, R. Glynne, D. C. Tully and A. K. Chatterjee, *J. Med. Chem.*, 2012, **55**, 4244–4273.
30 B. K. Park, N. R. Kitteringham and P. M. O'Neill, *Annu. Rev. Pharmacol. Toxicol.*, 2001, **41**, 443–470.
31 W. K. Hagman, *J. Med. Chem.*, 2008, **51**, 4359–4369.
32 H.-J. Böhm, D. Banner, S. Bendels, M. Kansy, B. Kuhn, K. Müller, U. Obst-Sander and M. Stahl, *ChemBioChem*, 2004, **5**, 637–643.
33 M. Moorjani, Z. Luo, E. Lin, B. G. Vong, Y. Chen, X. Zhang, J. K. Rueter, R. S. Gross, M. C. Lanier, J. E. Tellew, J. P. Williams, S. M. Lechner, S. Malany, M. Santos, M. I. Crespo, J. L. Díaz, J. Saunders and D. H. Slee, *Bioorg. Med. Chem. Lett.*, 2008, **18**, 5402–5405.
34 V. Mascitti, B. D. Stevens, C. Choi, K. F. McClure, C. R. W. Guimarães, K. A. Farley, M. J. Munchhof, R. P. Robinson, K. Futatsugi, S. Y. Lavergne, B. A. Lefker, P. Cornelius, P. D. Bonin, A. S. Kalgutkar, R. Sharma and Y. Chen, *Bioorg. Med. Chem. Lett.*, 2011, **21**, 1306–1309.
35 A. B. Eldrup, F. Soleymanzadeh, S. J. Taylor, I. Muegge, N. A. Farrow, D. Joseph, K. McKellop, C. Man, A. Kukulka and S. De Lombaert, *J. Med. Chem.*, 2009, **52**, 5880–5895.
36 C. S. Burgey, K. A. Robinson, T. A. Lyle, P. E. J. Sanderson, S. D. Lewis, B. J. Lucas, J. A. Krueger, R. Singh, C. Miller-Stein, R. A. White, B. Wong, E. A. Lyle, P. D. Williams, C. A. Coburn, B. D. Dorsey, J. C. Barrow, M. T. Stranieri, M. A. Holahan, G. R. Sitko, J. J. Cook, D. R. McMasters, C. M. McDonough, W. M. Sanders, A. A. Wallace, F. C. Clayton, D. Bohn, Y. M. Leonard, T. J. Detwiler, Jr, J. J. Lynch, Jr, Y. Yan, Z. Chen, L. Kuo, S. J. Gardell, J. A. Shafer and J. P. Vacca, *J. Med. Chem.*, 2003, **46**, 461–473.
37 M. B. Fisher, K. R. Henne and J. Boer, *Curr. Opin. Drug Discovery Dev.*, 2006, **9**, 101–109.
38 Auspex Pharmaceuticals, http://www.auspexpharma.com/auspex_SD254.html.
39 T. V. Magee, S. L. Ripp, B. Li, R. A. Buzon, L. Chupak, T. J. Dougherty, S. M. Finegan, D. Girard, A. E. Hagen, M. J. Falcone, K. A. Farley, K. Granskog, J. R. Hardink, M. D. Huband, B. J. Kamicker, T. Kaneko, M. J. Knickerbocker, J. L. Liras, A. Marra, I. Medina, T. T. Nguyen, M. C. Noe, R. S. Obach, J. P. O'Donnell, J. B. Penzien, U. D. Reilly, J. R. Schafer, Y. Shen, G. G. Stone, T. J. Strelevitz, J. Sun, A. Tait-Kamradt, A. D. Vaz, D. A. Whipple, D. W. Widlicka, D. G. Wishka, J. P. Wolkowski and M. E. Flanagan, *J. Med. Chem.*, 2009, **52**, 7446–7457.
40 C. M. Dixon, G. R. Park and M. H. Tarbit, *Biochem. Pharmacol.*, 1994, **47**, 1253–1257.
41 J. D. McEnroe and J. C. Fleishaker, *Clin. Pharmacokinet.*, 2005, **44**, 237–246.
42 K. P. Vyas, R. A. Halpin, L. A. Geer, J. D. Ellis, L. Liu, H. Cheng, C. Chavez-Eng, B. K. Matuszewski, S. L. Varga, A. R. Guiblin and J. D. Rogers, *Drug Metab. Dispos.*, 2000, **28**, 89–95.
43 M. J. Wild, D. McKillop and C. J. Butters, *Xenobiotica*, 1999, **29**, 847–857.
44 D. C. Evans, D. O'Conner, B. G. Lake, R. Evers, C. Allen and R. Hargreaves, *Drug Metab. Dispos.*, 2003, **31**, 861–869.

45 P. Buchan, C. Keywood, A. Wade and C. Ward, *Headache*, 2002, **42**(suppl. 2), S54–S62.
46 P. Tfelt-Hansen, P. De Vries and P. R. Saxena, *Drugs*, 2000, **60**, 1259–1287.
47 P. Jancova, P. Anzenbacher and E. Anzenbacherova, *Biomed. Pap. Med. Fac. Univ. Palacky Olomouc Czech Repub.*, 2010, **154**, 103–116.
48 W. Honma, M. Shimada, H. Sasano, S. Ozawa, M. Miyata, K. Nagata, T. Ikeda and Y. Yamazoe, *Drug Metab. Dispos.*, 2002, **30**, 944–949.
49 Y. Masubuchi, *Drug Metab. Pharmacokinet.*, 2006, **21**, 347–356.
50 A. O. Stewart, P. A. Bhatia, J. G. Martin, J. B. Summers, K. E. Rodriques, M. B. Martin, J. H. Holms, J. L. Moore, R. A. Craig, T. Kolasa, J. D. Ratajczyk, H. Mazdiyasni, F. A. Kerdesky, S. L. DeNinno, R. G. Maki, J. B. Bouska, P. R. Young, C. Lanni, R. L. Bell, G. W. Carter and C. D. Brooks, *J. Med. Chem.*, 1997, **40**, 1955–1968.
51 J. J. Bouska, R. L. Bell, C. L. Goodfellow, A. O. Stewart, C. D. Brooks and G. W. Carter, *Drug Metab. Dispos.*, 1997, **25**, 1032–1038.
52 W. M. Awni, R. A. Braeckman, G. R. Granneman, G. Witt and L. M. Dube, *Clin. Pharmacokinet.*, 1995, **29**(suppl. 2), 22–33.
53 V. Mascitti, T. S. Maurer, R. P. Robinson, J. Bian, C. M. Boustany-Kari, T. Brandt, B. M. Collman, A. S. Kalgutkar, M. K. Klenotic, M. T. Leininger, A. Lowe, R. J. Maguire, V. M. Masterson, Z. Miao, E. Mukaiyama, J. D. Patel, J. C. Pettersen, C. Preville, B. Samas, L. She, Z. Sobol, C. M. Steppan, B. D. Stevens, B. A. Thuma, M. Tugnait, D. Zeng and T. Zhu, *J. Med. Chem.*, 2011, **54**, 2952–2960.
54 A. S. Kalgutkar, M. Tugnait, T. Zhu, E. Kimito, Z. Miao, V. Mascitti, X. Yang, B. Tan, R. L. Walsky, J. Chupka, B. Feng and R. P. Robinson, *Drug Metab. Dispos.*, 2011, **39**, 1609–1619.
55 K. Beaumont, R. Webster, I. Gardner and K. Dack, *Curr. Drug Metab.*, 2003, **4**, 461–485.
56 K. M. Huttunen, H. Raunio and J. Rautio, *Pharmacol. Rev.*, 2011, **63**, 750–771.
57 H. Eng, M. Niosi, T. S. McDonald, A. Wolford, Y. Chen, S. T. Simila, J. N. Bauman, J. Warmus and A. S. Kalgutkar, *Xenobiotica*, 2010, **40**, 369–380.
58 T. Fujimoto, Y. Imaeda, N. Konishi, K. Hiroe, M. Kawamura, G. P. Textor, K. Aertgeerts and K. Kubo, *J. Med. Chem.*, 2010, **53**, 3517–3531.
59 T. Fujimoto, M. Tobisu, N. Konishi, M. Kawamura, N. Tada, T. Takagi and K. Kubo, *Bioorg. Med. Chem.*, 2009, **17**, 7993–8002.
60 T. D. Penning, J. J. Talley, S. R. Bertenshaw, J. S. Carter, P. W. Collins, S. Docter, M. J. Graneto, L. F. Lee, J. W. Malecha, R. S. Rogers, D. J. Rogier, S. S. Yu, G. D. Anderson, E. G. Burton, J. N. Cogburn, S. A. Gregory, C. M. Koboldt, W. E. Perkins, K. Seibert, A. W. Veenhuizen, Y. Y. Zhang and P. C. Isakson, *J. Med. Chem.*, 1997, **40**, 1347–1365.
61 J. A. Southers, J. N. Bauman, D. A. Price, P. S. Humphries, G. Balan, J. F. Sagal, T. S. Maurer, Y. Zhang, R. Oliver, M. Herr, D. R. Healy, M. Li, B. Kapinos, G. D. Fate, K. A. Riccardi, V. M. Paralkar, T. A. Brown and A. S. Kalgutkar, *ACS Med. Chem. Lett.*, 2010, **1**, 219–223.
62 D. S. Middleton, M. Andrews, P. Glossop, G. Gymer, D. Hepworth, A. Jessiman, P. S. Johnson, M. MacKenny, A. Stobie, K. Tang, P. Morgan and B. Jones, *Bioorg. Med. Chem. Lett.*, 2008, **18**, 5303–5306.
63 K. L. Dobo, R. S. Obach, D. Luffer-Atlas and J. P. Bercu, *Chem. Res. Toxicol.*, 2009, **22**, 348–356.
64 S. T. Orr, S. L. Ripp, T. E. Ballard, J. L. Henderson, D. O. Scott, R. S. Obach, H. Sun and A. S. Kalgutkar, *J. Med. Chem.*, 2012, **55**, 4896–4933.
65 A. F. Stepan, D. P. Walker, J. Bauman, D. A. Price, T. A. Baillie, A. S. Kalgutkar and M. D. Aleo, *Chem. Res. Toxicol.*, 2011, **24**, 1345–1410.
66 B. K. Park, A. Boobis, S. Clarke, C. E. Goldring, D. Jones, J. G. Kenna, C. Lambert, H. G. Laverty, D. J. Naisbitt, S. Nelson, D. A. Nicoll-Griffith, R. S. Obach, P. Routledge, D. A. Smith, D. J. Tweedie, N. Vermeulen, D. P. Williams, I. D. Wilson and T. A. Baillie, *Nat. Rev. Drug Discovery*, 2011, **10**, 292–306.
67 F. P. Guengerich and J. S. MacDonald, *Chem. Res. Toxicol.*, 2007, **20**, 344–369.
68 A. S. Kalgutkar, D. K. Dalvie, J. Aubrecht, E. B. Smith, S. L. Coffing, J. R. Cheung, C. Vage, M. E. Lame, P. Chiang, K. F. McClure, T. S. Maurer, R. V. Coelho, Jr, V. F. Soliman and K. Schildknegt, *Drug Metab. Dispos.*, 2007, **35**, 848–858.
69 A. S. Kalgutkar, J. N. Bauman, K. F. McClure, J. Aubrecht, S. R. Cortina and J. Paralkar, *Bioorg. Med. Chem. Lett.*, 2009, **19**, 1559–1563.
70 H. Chen, J. Murray, B. Kornberg, L. Dethloff, D. Rock, S. Nikam and A. E. Mutlib, *Chem. Res. Toxicol.*, 2006, **19**, 1341–1350.
71 H. K. Lim, J. Chen, C. Sensenhauser, K. Cook, R. Preston, T. Thomas, B. Shook, P. F. Jackson, S. Rassnick, K. Rhodes, V. Gopaul, R. Salter, J. Silva and D. C. Evans, *Chem. Res. Toxicol.*, 2011, **24**, 1012–1030.
72 P. R. Ortiz de Montellano, K. L. Kunze, G. S. Yost and B. A. Mico, *Proc. Natl. Acad. Sci. U. S. A.*, 1979, **76**, 746–749.
73 H. L. Lin, U. M. Kent and P. F. Hollenberg, *J. Pharmacol. Exp. Ther.*, 2002, **301**, 160–167.
74 H. S. Purba, J. L. Maggs, M. L. Orme, D. J. Back and B. K. Park, *Br. J. Clin. Pharmacol.*, 1987, **23**, 447–453.
75 S. Nakayama, R. Atsumi, H. Takakusa, Y. Kobayashi, A. Kurihara, Y. Nagai, D. Nakai and O. Okazaki, *Drug Metab. Dispos.*, 2009, **37**, 1970–1977.
76 S. M. Westaway, S. L. Brown, S. C. M. Fell, C. N. Johnson, D. T. MacPherson, D. J. Mitchell, J. W. Myatt, S. J. Stanway, J. T. Seal, G. Stemp, M. Thompson, K. Lawless, F. McKay, A. I. Muir, J. M. Barford, C. Cluff, S. R. Mahmood, K. L. Matthews, S. Mohamed, B. Smith, A. J. Stevens, V. J. Bolton, E. M. Jarvie and G. J. Sanger, *J. Med. Chem.*, 2009, **52**, 1180–1189.

77 Z. Zhao, W. H. Leister, J. A. O'Brien, W. Lemaire, D. L. Williams, Jr, M. A. Jacobson, C. Sur, G. G. Kinney, D. J. Pettibone, P. R. Tiller, S. Smith, G. D. Hartman, C. W. Lindsley and S. E. Wolkenberg, *Bioorg. Med. Chem. Lett.*, 2009, **19**, 1488–1491.
78 M. K. Wendt and W. P. Schiemann, *Breast Cancer Res.*, 2009, **11**, R68.
79 D. P. Walker, F. C. Bi, A. S. Kalgutkar, J. N. Bauman, S. X. Zhao, J. R. Soglia, G. E. Aspnes, D. W. Kung, J. Klug-McLeod, M. P. Zawistoski, M. A. McGlynn, R. Oliver, M. Dunn, J. C. Li, D. T. Richter, B. A. Cooper, J. C. Kath, C. A. Hulford, C. L. Autry, M. J. Luzzio, E. J. Ung, W. G. Roberts, P. C. Bonnette, L. Buckbinder, A. Mistry, M. C. Griffor, S. Han and A. Guzman-Perez, *Bioorg. Med. Chem. Lett.*, 2008, **18**, 6071–6077.
80 K. M. Bertelsen, K. Venkatakrishnan, L. L. Von Moltke, R. S. Obach and D. J. Greenblatt, *Drug Metab. Dispos.*, 2003, **31**, 289–293.
81 M. Murray, *Curr. Drug Metab.*, 2000, **1**, 67–84.
82 C. M. Kaye, R. E. Haddock, P. F. Langley, G. Mellows, T. C. Tasker, B. D. Zussman and W. H. Greb, *Acta Psychiatr. Scand., Suppl.*, 1989, **350**, 60–75.
83 A. Hemeryck, R. A. Lefebyre, C. De Vriendt and F. M. Belpaire, *Clin. Pharmacol. Ther.*, 2000, **67**, 283–291.
84 E. Spina, A. Avenoso, G. Facciola, M. G. Scordo, M. Ancione and A. Madia, *Ther. Drug Monit.*, 2001, **23**, 223–227.
85 D. J. Belle, C. S. Ernest, J. M. Sauer, B. P. Smith, H. R. Thomasson and J. W. Witcher, *J. Clin. Pharmacol.*, 2002, **42**, 1219–1227.
86 A. T. Yarnell, http://pubs.acs.org/cen/science/87/8725scil.html.
87 A. S. Kalgutkar and M. T. Didiuk, *Chem. Biodiversity*, 2009, **6**, 2115–2137.
88 R. S. Obach, A. S. Kalgutkar, T. F. Ryder and G. S. Walker, *Chem. Res. Toxicol.*, 2008, **21**, 1890–1899.
89 W. K. Hagmann, *Arch. Pharm.*, 2008, **341**, 405–411.
90 R. Sarabu, F. T. Bizzarro, W. L. Corbett, M. T. Dvorozniak, W. Geng, J. F. Grippo, N.-E. Haynes, S. Hutchings, L. Garofalo, K. R. Guertin, D. W. Hilliard, M. Kabat, R. F. Kester, W. Ka, Z. Liang, P. E. Mahaney, L. Marcus, F. M. Matschinsky, D. Moore, J. Racha, R. Radinov, Y. Ren, L. Qi, M. Pignatello, C. L. Spence, T. Steele, J. Tengi and J. Grimsby, *J. Med. Chem.*, 2012, **55**, 7021–7036.
91 J. A. Pfefferkorn, J. Lou, M. L. Minich, K. J. Filipski, M. He, R. Zhou, S. Ahmed, J. Benbow, A. G. Perez, M. Tu, J. Litchfield, R. Sharma, K. Metzler, F. Bourbonais, C. Huang, D. A. Beebe and P. J. Oates, *Bioorg. Med. Chem. Lett.*, 2009, **19**, 3247–3252.
92 J. Litchfield, R. Sharma, K. Atkinson, K. J. Filipski, S. W. Wright, J. A. Pfefferkorn, B. Tan, R. E. Kosa, B. Stevens, M. Tu and A. S. Kalgutkar, *Bioorg. Med. Chem. Lett.*, 2010, **20**, 6262–6267.
93 J. A. Pfefferkorn, A. Guzman-Perez, P. J. Oates, J. Litchfield, G. Aspnes, A. Basak, J. Benbow, M. A. Berliner, J. Bian, C. Choi, K. Freeman-Cook, J. W. Corbett, M. Didiuk, J. R. Dunetz, K. J. Filipski, W. M. Hungerford, C. S. Jones, K. Karki, A. Ling, J.-C. Li, L. Patel, C. Perreault, H. Risley, J. Saenz, W. Song, M. Tu, R. Aiello, K. Atkinson, N. Barucci, D. Beebe, P. Bourassa, F. Bourbounais, A. M. Brodeur, R. Burbey, J. Chen, T. D'Aquila, D. R. Derksen, N. Haddish-Berhane, C. Huang, J. Landro, A. L. Lapworth, M. MacDougall, D. Perregaux, J. Pettersen, A. Robertson, B. Tan, J. L. Treadway, S. Liu, X. Qiu, J. Knafels, M. Ammirati, X. Song, P. DaSilva-Jardine, S. Liras, L. Sweet and T. P. Rolph, *Med. Chem. Commun.*, 2011, **2**, 828–839.
94 E. F. Mesaros, T. V. Thieu, G. J. Wells, C. A. Zificsak, J. C. Wagner, H. J. Breslin, R. Tripathy, J. L. Diebold, R. J. McHugh, A. T. Wohler, M. R. Quail, W. Wan, L. Lu, Z. Huang, M. S. Albom, T. S. Angeles, K. J. Wells-Knecht, L. D. Aimone, M. Cheng, M. A. Ator, G. R. Ott and B. D. Dorsey, *J. Med. Chem.*, 2012, **55**, 115–125.
95 K. J. Wells-Knecht, G. R. Ott, M. Cheng, G. J. Wells, H. J. Breslin, D. E. Gingrich, L. Weinberg, E. F. Mesaros, Z. Huang, M. Yazdanian, M. A. Ator, L. D. Aimone, K. Zeigler and B. D. Dorsey, *Chem. Res. Toxicol.*, 2011, **24**, 1994–2003.
96 A. Fura, Y.-Z. Shu, M. Shu, R. L. Hanson, V. Roongta and W. Griffith Humphreys, *J. Med. Chem.*, 2004, **47**, 4339–4351.
97 A. E. Buhl, D. J. Waldon, C. A. Baker and G. A. Johnson, *J. Invest. Dermatol.*, 1990, **95**, 553–557.
98 J. M. Pereillo, M. Maftouh, A. Andrieu, M. F. Uzabiaga, O. Fedeli, P. Savi, M. Pascal, J. M. Herbert, J. P. Maffrand and C. Picard, *Drug Metab. Dispos.*, 2002, **30**, 1288–1295.
99 P. Savi and J. M. Herbert, *Semin. Thromb. Hemostasis*, 2005, **31**, 174–183.
100 A. Markham and A. J. Wagstaff, *Drugs*, 1998, **55**, 269–274.
101 C. H. Yun, R. A. Okerholm and F. P. Guengerich, *Drug Metab. Dispos.*, 1993, **21**, 403–409.
102 J. K. Crane and H. T. Shih, *Am. J. Med.*, 1993, **95**, 445–446.
103 N. Yumibe, K. Huie, K. J. Chen, M. Snow, R. P. Clement and M. N. Cayen, *Biochem. Pharmacol.*, 1996, **51**, 165–172.
104 C. U. Pae, *Expert Opin. Pharmacother.*, 2009, **10**, 875–887.
105 J. W. Clader, *J. Med. Chem.*, 2004, **47**, 1–9.
106 A. N. Nedderman, G. J. Dear, S. North, R. S. Obach and D. Higton, *Xenobiotica*, 2011, **41**, 605–622.
107 F. P. Guengerich, *Chem. Res. Toxicol.*, 2009, **22**, 237–238.
108 L. Leclercq, F. Cuyckens, G. S. Mannens, R. de Vries, P. Timmerman and D. C. Evans, *Chem. Res. Toxicol.*, 2009, **22**, 280–293.
109 R. A. Hartz, V. T. Ahuja, X. Zhuo, R. J. Mattson, D. J. Denhart, J. A. Deskus, V. M. Vrudhula, S. Pan, J. L. Ditta, Y. Z. Shu, J. E. Grace, K. A. Lentz, S. Lelas, Y. W. Li, T. F. Molski, S. Krishnananthan, H. Wong, J. Qian-Cutrone, R. Schartman, R. Denton, N. J. Lodge, R. Zaczek, J. E. Macor and J. J. Bronson, *J. Med. Chem.*, 2009, **52**, 7653–7668.
110 P. M. O'Neill, B. K. Park, A. E. Shone, J. L. Maggs, P. Roberts, P. A. Stocks, G. A. Biagini, P. G. Bray, P. Gibbons, N. Berry, P. A. Winstanley, A. Mukhtar, R. Bonar-Law, S. Hindley, R. B. Bambal, C. B. Davis, M. Bates, T. K. Hart, S. L. Gresham, R. M. Lawrence, R. A. Brigandi, F. M. Gomez-delas-Heras, D. V. Gargallo and S. A. Ward, *J. Med. Chem.*, 2009, **52**, 1408–1415.
111 A. S. Kalgutkar, J. Driscoll, S. X. Zhao, G. S. Walker, R. M. Shepard, J. R. Soglia, J. Atherton, L. Yu,

A. E. Mutlib, M. J. Munchhof, L. A. Reiter, C. S. Jones, J. L. Doty, K. A. Trevena, C. L. Shaffer and S. L. Ripp, *Chem. Res. Toxicol.*, 2007, **20**, 1954–1965.

112 H. J. Finlay, J. Lloyd, W. Vaccaro, A. Kover, L. Yan, G. Bhave, J. Prol, T. Huynh, R. Bhandaru, Y. Caringal, J. DiMarco, J. Gan, T. Harper, C. Huang, M. L. Conder, H. Sun, P. Levesque, M. Blanar, K. Atwal and R. Wexler, *J. Med. Chem.*, 2012, **55**, 3036–3048.

113 C. D. Cox, P. J. Coleman, M. J. Breslin, D. B. Whitman, R. M. Garbaccio, M. E. Fraley, C. A. Buser, E. S. Walsh, K. Hamilton, M. D. Schaber, R. B. Lobell, W. Tao, J. P. Davide, R. E. Diehl, M. T. Abrams, V. J. South, H. E. Huber, M. Torrent, T. Pruekasritanont, C. Li, D. E. Slaughter, E. Mahan, C. Fernandez-Metzler, Y. Yan, L. C. Kuo, N. E. Kohl and G. D. Hartman, *J. Med. Chem.*, 2008, **51**, 4239–4252.